Towards stabilization-free Hybrid High-Order methods for elliptic problems

Towards stabilization-free Hybrid High-Order methods for elliptic problems

Andrea Borio* Karol L. Cascavita * Matteo Cicuttin *,† Francesca Marcon*

July 23, 2025

Abstract

We devise and study Hybrid High-Order (HHO) methods in a *stabilization-free* formulation, i.e. based on discrete bilinear forms not requiring an additional, explicit stabilization term. The discretization hinges on newly defined reconstruction operators mapping on polynomial spaces richer than the ones used in standard HHO literature. Optimal order a priori error estimates are obtained with the expected HHO convergence rates. The well-posedness of the discrete scheme is currently only conjectured. Extensive numerical tests are presented, supporting the stability and robustness of the new methods and shedding a light on future theoretical developments.

Keywords Hybrid High-Order methods; stabilization-free; reconstruction operators

1 Introduction

Hybrid High-Order (HHO) methods were introduced in [30, 31] as a new method in the class of Discontinuous Skeletal discretizations. In the last decade HHO methods enjoyed broad acceptance, especially in the field of computational mechanics. An incomplete list of successful applications includes works in solid mechanics [1, 23], obstacle problems [16, 22], unfitted interfaces [11], fluid mechanics [15, 9], poromechanics [17, 10], electromagnetics [18, 25], acoustics [12] and eigenproblems [14, 13]. The main features of HHO are the approximation of the solution with arbitrary order polynomials, support for fully polytopal meshes and easy *hp*-refinement. The HHO unknowns are placed both in the cells and on the faces of the mesh, in order to approximate a pair including the primal variable in the cells and its trace on the skeleton. In particular, these unknowns are used (i) by a reconstruction operator, which reconstructs a high-order field in the cell and (ii) by a stabilization operator, which weakly enforces in each mesh cell the matching of the traces of the cell functions with the face unknowns. These two operators are then combined in a local bilinear form which, after local static condensation, is assembled into a global problem posed only on the face unknowns. The mathematical foundations, together with multiple applications, are discussed extensively in [24, 28], whereas implementation details are described in [21].

Multiple bridges between HHO and other methods of the Discontinuous Skeletal family have been established in the past years. For example, in [31], a connection was made between the lowest-order HHO method, the Hybrid Finite Volume method from [35] and subsequently the Hybrid Mimetic Mixed methods from [32]. Subsequently, HHO methods were linked to Hybridizable Discontinuous Galerkin (HDG) methods, Virtual Element Methods (VEM) and Weak Galerkin (WG) methods [26, 27, 39].

In recent years, the study of Galerkin methods suitable for polytopal meshes that avoid the use of a non-physical stabilization term has attracted the interest of the scientific community. The importance of stabilization-free polytopal methods is well known, especially in the context of nonlinear problems [37, 1] and eigenproblems [6, 7, 40]. In particular, in the framework of VEM, recent studies proposed polygonal

*Dipartimento di Scienze Matematiche, Politecnico di Torino, Corso Duca degli Abruzzi 24, 10129, Torino, Italy.
† Corresponding author, matteo.cicuttin@polito.it

numerical schemes based on the definition of bilinear forms that involve only polynomial projections of virtual functions. The reader can refer to [33, 19, 41, 5, 8] for numerical explorations in computational mechanics and to [38, 3, 4, 2] for more theoretical works. In the context of HHO, stabilization-free variants exist and are based on the use of spaces from the Raviart-Thomas (RT) family. In particular, local RT-Nédélec spaces on simplicial submeshes were exploited in [29]. In addition, in [1] RT spaces on simplicial meshes were employed, though optimal convergence was not attained. In WG context, a "superconvergent stabilizer-free" method for general meshes has been recently described in [42], also based on RT spaces on local submeshes.

In this work we introduce and study numerically a variant of HHO for elliptic problems, posed on 2D and 3D polytopal domains and free of an explicit stabilization term. The proposed variant preserves optimal HHO convergence rates and is based on introducing modified reconstruction operators mapping on polynomial spaces richer than the ones used in standard HHO methods.

In the following let Ω be an open, bounded, connected, Lipschitz subset of $\mathbb{R}^d$ and $f \in \mathrm{L}^2(\Omega)$. We consider the problem of finding $u \in V := \mathrm{H}^1_0(\Omega)$ such that

$$(\nabla u, \nabla v)_\Omega = (f, v)_\Omega\,, \qquad \forall v \in V\,, \tag{1}$$

where $(\cdot,\cdot)_\zeta$ denotes the $\mathrm{L}^2(\zeta)$-scalar product for any $\zeta \subset \mathbb{R}^d$. In Section 2 we describe the numerical scheme and state the discrete problem, discussing its well-posedness. In Section 3 we derive optimal order a priori error estimates. Finally, in Section 4 we show the results of some numerical tests assessing stability and convergence of the proposed method.

Throughout the paper, $\mathbb{P}^k_d(\zeta)$ denotes the space of polynomials up to degree k defined on ζ, for $\zeta \subset \mathbb{R}^d$. Inside the proofs C denotes a generic constant, independent of the mesh size and that can be different at each occurrence.

2 Discrete setting

The goal of this section is to illustrate briefly the setting to devise HHO and subsequently to introduce the stabilization-free variant. The domain Ω is assumed to be discretized with a mesh fulfilling the standard HHO assumptions [31, 30] and in the following, let $\mathcal{T}_h$ denote the set of the mesh cells, $\mathcal{F}_h$ the set of mesh faces, and $\mathcal{F}_h^b$ the boundary faces. In addition, for each element $T \in \mathcal{T}_h$, $\mathcal{F}^T$ denotes the set of all faces $F \subset \partial T$. For each $T \in \mathcal{T}_h$, h_T denotes the diameter of T and let $h = \max_{T \in \mathcal{T}_h} h_T$.

2.1 HHO spaces and standard operators

Given an element $T \in \mathcal{T}_h$, the HHO(k', k) method attaches polynomials of degree $k' \geqslant 0$ to the interior of T and polynomials of degree $k \geqslant 0$ to the faces of T, with the constraint that $k' \in \{k-1, k, k+1\}$ (therefore the HHO$(k-1,k)$ method requires $k \geqslant 1$). These polynomials are collected to form the element-local space

$$\underline{\mathsf{U}}_T^{k',k} := \mathbb{P}^{k'}_d(T) \times \mathbb{P}^k_{d-1}(\mathcal{F}^T), \qquad \mathbb{P}^k_{d-1}(\mathcal{F}^T) := \bigtimes_{F \in \mathcal{F}^T} \mathbb{P}^k_{d-1}(F).$$

A generic member of $\underline{\mathsf{U}}_T^{k',k}$ is denoted as $\underline{\mathsf{v}}_T := (\mathsf{v}_T, \mathsf{v}_{\partial T})$ and further $\mathsf{v}_F := \mathsf{v}_{\partial T}|_F$, $\forall F \in \mathcal{F}^T$. For a polygon T with N_T^∂ faces, the space $\underline{\mathsf{U}}_T^{k',k}$ has dimension

$$N_T^{k',k} := \dim(\mathbb{P}^{k'}_d(T)) + \dim(\mathbb{P}^k_{d-1}(\mathcal{F}^T)), \tag{2}$$

with $\dim(\mathbb{P}^{k'}_d(T)) = \binom{k'+d}{d}$ and $\dim(\mathbb{P}^k_{d-1}(\mathcal{F}^T)) = N_T^\partial \binom{k+d-1}{d-1}$.
The global HHO(k', k) space is obtained by collecting all the element-based unknowns as

$$\underline{\mathsf{U}}_h^{k',k} := \left\{ \bigtimes_{T \in \mathcal{T}_h} \mathbb{P}^{k'}_d(T) \right\} \times \left\{ \bigtimes_{F \in \mathcal{F}_h} \mathbb{P}^k_{d-1}(F) \right\},$$

where we remark that the face-based unknowns are single-valued polynomials, but discontinuous on the vertices. Homogeneous Dirichlet boundary conditions are enforced by strongly setting to zero the unknowns associated to the boundary faces, which results in the space

$$\underline{\mathsf{U}}_{h,0}^{k',k} := \left\{ \underline{\mathsf{v}}_h = ((\mathsf{v}_T)_{T\in\mathcal{T}_h}, (\mathsf{v}_F)_{F\in\mathcal{F}_h}) \in \underline{\mathsf{U}}_h^{k',k} | \ \mathsf{v}_F = 0, \quad \forall F \in \mathcal{F}_h^b \right\}.$$

More general boundary conditions can be applied, see for example [24, Section 8.5]. For a given $T \in \mathcal{T}_h$, the space $\underline{\mathsf{U}}_T^{k',k}$ is endowed with the following local semi-norm:

$$|\underline{\mathsf{v}}_T|^2_{\underline{\mathsf{U}}_T^{k',k}} := \|\nabla \mathsf{v}_T\|^2_{\mathrm{L}^2(T)} + h_T^{-1} \|\mathsf{v}_T - \mathsf{v}_{\partial T}\|^2_{\mathrm{L}^2(\partial T)}, \quad \forall \underline{\mathsf{v}}_T := (\mathsf{v}_T, \mathsf{v}_{\partial T}) \in \underline{\mathsf{U}}_T^{k',k}. \tag{3}$$

Summing up local seminorms we obtain a norm for $\underline{\mathsf{U}}_{h,0}^{k',k}$:

$$\|\underline{\mathsf{v}}_h\|^2_{\underline{\mathsf{U}}_{h,0}^{k',k}} := \sum_{T\in\mathcal{T}_h} |\underline{\mathsf{v}}_T|^2_{\underline{\mathsf{U}}_T^{k',k}}, \quad \forall \underline{\mathsf{v}}_h \in \underline{\mathsf{U}}_{h,0}^{k',k}. \tag{4}$$

2.1.1 Reduction operator

Generic functions of $\mathrm{H}^1(\Omega)$ are reduced to elements of $\underline{\mathsf{U}}_h^{k',k}$ by using standard L^2-projections: let $T \in \mathcal{T}_h$, we define for each $v \in \mathrm{L}^2(T)$ and for each $w \in \mathrm{L}^2(\partial T)$ the cell-based and face-based L^2-orthogonal projections $\pi_T^{k'} : \mathrm{L}^2(T) \to \mathbb{P}_d^{k'}(T)$ and $\pi_{\partial T}^k : \mathrm{L}^2(\partial T) \to \mathbb{P}_{d-1}^k(\mathcal{F}^T)$ respectively, such that

$$(\pi_T^{k'} v - v, p)_T = 0, \quad \forall p \in \mathbb{P}_d^{k'}(T), \tag{5}$$

$$(\pi_{\partial T}^k w - w, q)_{\partial T} = 0, \quad \forall q \in \mathbb{P}_{d-1}^k(\mathcal{F}^T). \tag{6}$$

Using the L^2-projectors we define the *local reduction operator* $\underline{\mathsf{I}}_T^{k',k} : \mathrm{H}^1(T) \to \underline{\mathsf{U}}_T^{k',k}$ of a function $v \in \mathrm{H}^1(T)$ as

$$\underline{\mathsf{I}}_T^{k',k}(v) := (\pi_T^{k'} v, \pi_{\partial T}^k v), \tag{7}$$

and the *global reduction operator* $\underline{\mathsf{I}}_h^{k',k} : \mathrm{H}^1(\Omega) \to \underline{\mathsf{U}}_h^{k',k}$ such that $\underline{\mathsf{I}}_h^{k',k}(v)_{|T} = \underline{\mathsf{I}}_T^{k',k}(v) \in \underline{\mathsf{U}}_T^{k',k}$ for all $v \in \mathrm{H}^1(\Omega)$ and for all $T \in \mathcal{T}_h$.

Lemma 1. *Let $T \in \mathcal{T}_h$ and $v \in \mathrm{H}^1(T)$ be given. Then, there exists $C > 0$ independent of h_T such that*

$$\left| \underline{\mathsf{I}}_T^{k',k}(v) \right|_{\underline{\mathsf{U}}_T^{k',k}} \leqslant C \|\nabla v\|_{\mathrm{L}^2(T)}. \tag{8}$$

Proof. By the definition of the seminorm in (3) and the triangle inequality,

$$\begin{aligned}
\left| \underline{\mathsf{I}}_T^{k',k}(v) \right|^2_{\underline{\mathsf{U}}_T^{k',k}} &= \left\| \nabla \pi_T^{k'} v \right\|^2_{\mathrm{L}^2(T)} + h_T^{-1} \left\| \pi_T^{k'} v - \pi_{\partial T}^k v \right\|^2_{\mathrm{L}^2(\partial T)} \\
&= \left\| \nabla \pi_T^{k'} v \right\|^2_{\mathrm{L}^2(T)} + h_T^{-1} \left\| \pi_T^{k'} v - \pi_T^0 v + \pi_T^0 v - \pi_{\partial T}^k v \right\|^2_{\mathrm{L}^2(\partial T)} \\
&\leqslant \left\| \nabla \pi_T^{k'} v \right\|^2_{\mathrm{L}^2(T)} + 2h_T^{-1} \left(\left\| \pi_T^{k'} (v - \pi_T^0 v) \right\|^2_{\mathrm{L}^2(\partial T)} + \left\| \pi_{\partial T}^k (v - \pi_T^0 v) \right\|^2_{\mathrm{L}^2(\partial T)} \right).
\end{aligned}$$

Then, (8) is obtained by discrete trace inequalities, the continuity of orthogonal projection operators and

Poincaré inequalities:

$$
\begin{aligned}
\left\|\nabla \pi_T^{k'} v\right\|_{\mathrm{L}^2(T)} &\leqslant C\left\|\nabla v\right\|_{\mathrm{L}^2(T)}\,, \\
h_T^{-1}\left\|\pi_T^{k'}(v-\pi_T^0 v)\right\|_{\mathrm{L}^2(\partial T)}^2 &\leqslant C h_T^{-2}\left\|\pi_T^{k'}(v-\pi_T^0 v)\right\|_{\mathrm{L}^2(T)}^2 \\
&\leqslant C h_T^{-2}\left\|v-\pi_T^0 v\right\|_{\mathrm{L}^2(T)}^2 \leqslant C\left\|\nabla v\right\|_{\mathrm{L}^2(T)}^2\,, \\
h_T^{-1}\left\|\pi_{\partial T}^{k}(v-\pi_T^0 v)\right\|_{\mathrm{L}^2(\partial T)}^2 &\leqslant h_T^{-1}\left\|v-\pi_T^0 v\right\|_{\mathrm{L}^2(\partial T)}^2 \leqslant C h_T^{-2}\left\|v-\pi_T^0 v\right\|_{\mathrm{L}^2(T)}^2 \\
&\leqslant C\left\|\nabla v\right\|_{\mathrm{L}^2(T)}^2\,.
\end{aligned}
$$

□

2.1.2 Reconstruction operator

Let $\underline{\mathsf{v}}_T \in \underline{\mathsf{U}}_T^{k',k}$, we define the reconstruction operator $\mathsf{R}_T^{k',k} : \underline{\mathsf{U}}_T^{k',k} \to \mathbb{P}_d^{k+1}(T)$ as the solution of the well-posed Neumann problem

$$
\begin{cases}
(\nabla \mathsf{R}_T^{k',k}(\underline{\mathsf{v}}_T), \nabla q)_T = -(\mathsf{v}_T, \Delta q)_T + (\mathsf{v}_{\partial T}, \mathbf{n}\cdot\nabla q)_{\partial T}\,, & \forall q \in \mathbb{P}_d^{k+1}(T), \\
(\mathsf{R}_T^{k',k}(\underline{\mathsf{v}}_T), 1)_T = (\mathsf{v}_T, 1)_T\,, &
\end{cases}
\tag{9}
$$

where $\mathbf{n}$ denotes the unit outward normal to ∂T. In the following, we state some classical results about the operator $\mathsf{R}_T^{k',k}$ [24].

Lemma 2. *For all $p \in \mathbb{P}_d^{k+1}(T)$, $\mathsf{R}_T^{k',k}(\underline{\mathsf{I}}_T^{k',k}(p)) = p$.*

Lemma 3. *For all $v \in \mathrm{H}^1(T)$, the composed operator $\mathsf{E}_T^{k+1} := \mathsf{R}_T^{k',k} \circ \underline{\mathsf{I}}_T^{k',k}$ is the elliptic projection*

$$
\begin{cases}
(\nabla \mathsf{E}_T^{k+1}(v), \nabla q)_T = (\nabla v, \nabla q)_T\,, & \forall q \in \mathbb{P}_d^{k+1}(T), \\
(\mathsf{E}_T^{k+1}(v), 1)_T = (v, 1)_T. &
\end{cases}
\tag{10}
$$

Lemma 4. *Let $T \in \mathcal{T}_h$ be given. Let $k' \in \{k-1, k, k+1\}$ and let $\underline{\mathsf{v}}_T \in \underline{\mathsf{U}}_T^{k',k}$. Then, there exists $C > 0$ independent of h_T such that*

$$
\left\|\nabla \mathsf{R}_T^{k',k}(\underline{\mathsf{v}}_T)\right\|_{\mathrm{L}^2(T)} \leqslant C\left|\underline{\mathsf{v}}_T\right|_{\underline{\mathsf{U}}_T^{k',k}}\,. \tag{11}
$$

2.2 Stabilization-free HHO methods

Let $\mathbb{H}_d^{\ell}(T)$ be the space of d-variate harmonic polynomials of a given degree ℓ defined on T. For $\ell \geqslant 0$

$$
\tilde{\mathbb{P}}_d^{k',\ell}(T) := \left\{p \in \mathbb{P}_d^{k'+2+\ell}(T) \,|\, \Delta p \in \mathbb{P}_d^{k'}(T)\right\} = \mathbb{P}_d^{k'+2}(T) \oplus (\mathbb{H}_d^{k'+2+\ell}(T) \setminus \mathbb{H}_d^{k'+2}(T))\,,
$$

that is an enrichment of $\mathbb{P}_d^{k'+2}(T)$ with harmonic polynomials. The methods presented in the following are based on the definition of suitable reconstruction operators onto the space $\tilde{\mathbb{P}}_d^{k',\ell}(T)$. For any $T \in \mathcal{T}_h$, given a local integer $\ell \geqslant 0$, we define the operator $\tilde{\mathsf{R}}_{\ell,T}^{k',k} : \underline{\mathsf{U}}_T^{k',k} \to \tilde{\mathbb{P}}_d^{k',\ell}(T)$ such that, given $\underline{\mathsf{v}}_T \in \underline{\mathsf{U}}_T^{k',k}$,

$$
\begin{cases}
(\nabla \tilde{\mathsf{R}}_{\ell,T}^{k',k}(\underline{\mathsf{v}}_T), \nabla \tilde{q})_T = -(\mathsf{v}_T, \Delta \tilde{q})_T + (\mathsf{v}_{\partial T} - \mathcal{E}_{\partial T}^{k',k}(\underline{\mathsf{v}}_T), \mathbf{n}\cdot\nabla \tilde{q})_{\partial T}, & \forall \tilde{q} \in \tilde{\mathbb{P}}_d^{k',\ell}(T)\,, \\
(\tilde{\mathsf{R}}_{\ell,T}^{k',k}(\underline{\mathsf{v}}_T), 1)_T = (\mathsf{v}_T, 1)_T\,, &
\end{cases}
\tag{12}
$$

where

$$
\mathcal{E}_{\partial T}^{k',k}(\underline{\mathsf{v}}_T) := \begin{cases}
\pi_{\partial T}^{k} \mathsf{R}_T^{k',k}(\underline{\mathsf{v}}_T) - \mathsf{R}_T^{k',k}(\underline{\mathsf{v}}_T), & \text{if } k' \in \{k-1, k\}\,, \\
\pi_{\partial T}^{k} \mathsf{v}_T - \mathsf{v}_T, & \text{if } k' = k+1\,.
\end{cases}
\tag{13}
$$

In the following, we prove some key properties of $\tilde{\mathsf{R}}_{\ell,T}^{k',k}$.

Lemma 5. *Let $T \in \mathcal{T}_h$ and let $\tilde{\mathsf{R}}_{\ell,T}^{k',k}$ be the operator defined by* (12)*. Then, for any $p \in \mathbb{P}_d^{k+1}(T)$,*

$$\tilde{\mathsf{R}}_{\ell,T}^{k',k}(\underline{\mathsf{I}}_T^{k',k}(p)) = p\,.$$

Proof. First, by (13) and Lemma 2 , we get $\mathcal{E}_{\partial T}^{k',k}(\underline{\mathsf{I}}_T^{k',k}(p)) = \pi_{\partial T}^k p - p$. Looking at the first equation in (12), we get

$$\left(\nabla\tilde{\mathsf{R}}_{\ell,T}^{k',k}(\underline{\mathsf{I}}_T^{k',k}(p)), \nabla\tilde{q}\right)_T = -\,(p, \Delta\tilde{q})_T + \,(p, \mathbf{n}\cdot\nabla\tilde{q})_{\partial T} = \,(\nabla p, \nabla\tilde{q})_T\,, \quad \forall \tilde{q} \in \tilde{\mathbb{P}}_d^{k',\ell}(T)\,.$$

Choosing $\tilde{q} = \tilde{\mathsf{R}}_{\ell,T}^{k',k}(\underline{\mathsf{I}}_T^{k',k}(p)) - p$, we obtain

$$(\nabla\tilde{\mathsf{R}}_{\ell,T}^{k',k}(\underline{\mathsf{I}}_T^{k',k}(p)) - \nabla p, \nabla\tilde{q})_T = \left\|\nabla\left(\tilde{\mathsf{R}}_{\ell,T}^{k',k}(\underline{\mathsf{I}}_T^{k',k}(p)) - p\right)\right\|_{\mathrm{L}^2(T)}^2 = 0\,,$$

which implies $\tilde{\mathsf{R}}_{\ell,T}^{k',k}(\underline{\mathsf{I}}_T^{k',k}(p)) = p$ since $(\tilde{\mathsf{R}}_{\ell,T}^{k',k}(\underline{\mathsf{I}}_T^{k',k}(p)) - p, 1)_T = 0$. □

Lemma 6. *Let $T \in \mathcal{T}_h$ and let $\tilde{\mathsf{R}}_{\ell,T}^{k',k}$ be the operator defined by* (12)*. Then, for any $\underline{\mathsf{v}}_T \in \underline{\mathsf{U}}_T^{k',k}$,*

$$(\nabla\tilde{\mathsf{R}}_{\ell,T}^{k',k}(\underline{\mathsf{v}}_T), \nabla q)_T = (\nabla\mathsf{R}_T^{k',k}(\underline{\mathsf{v}}_T), \nabla q)_T \quad \forall q \in \mathbb{P}_d^{k+1}(T)\,. \tag{14}$$

Proof. Let $q \in \mathbb{P}_d^{k+1}(T)$. Since $\mathbf{n}\cdot\nabla q \in \mathbb{P}_{d-1}^k(\mathcal{F}^T)$, we get

$$\begin{aligned} 0 &= \left(\mathcal{E}_{\partial T}^{k',k}(\underline{\mathsf{v}}_T), \mathbf{n}\cdot\nabla q\right)_{\partial T} \\ &= \begin{cases} (\pi_{\partial T}^k \mathsf{R}_T^{k',k}(\underline{\mathsf{v}}_T) - \mathsf{R}_T^{k',k}(\underline{\mathsf{v}}_T), \mathbf{n}\cdot\nabla q)_{\partial T}, & \text{if } k' \in \{k-1, k\} \\ (\pi_{\partial T}^k \mathsf{v}_T - \mathsf{v}_T, \mathbf{n}\cdot\nabla q)_{\partial T}, & \text{if } k' = k+1 \end{cases} \end{aligned} \tag{15}$$

Then, by the definition of $\tilde{\mathsf{R}}_{\ell,T}^{k',k}$ (12), using (15), and since $\Delta q \in \mathbb{P}_d^{k-1}(T) \subseteq \mathbb{P}_d^{k'}(T)$, $\forall k' \in \{k-1, k, k+1\}$,

$$(\nabla\tilde{\mathsf{R}}_{\ell,T}^{k',k}(\underline{\mathsf{v}}_T), \nabla q)_T = -(\mathsf{v}_T, \Delta q)_T + (\mathsf{v}_{\partial T}, \mathbf{n}\cdot\nabla q)_{\partial T} = (\nabla\mathsf{R}_T^{k',k}(\underline{\mathsf{v}}_T), \nabla q)\,.$$

□

Remark 1. As a straightforward consequence of Lemma 6 we have the orthogonality: $\forall v \in \mathrm{H}^1(T)$,

$$\left(\nabla\tilde{\mathsf{R}}_{\ell,T}^{k',k}\left(\underline{\mathsf{I}}_T^{k',k}(v)\right), \nabla q\right)_T = \left(\nabla\mathsf{E}_T^{k+1}(v), \nabla q\right)_T = \,(\nabla v, \nabla q)_T\,, \quad \forall q \in \mathbb{P}_d^{k+1}(T)\,, \tag{16}$$

where $\mathsf{E}_T^{k+1} = \mathsf{R}_T^{k',k} \circ \underline{\mathsf{I}}_T^{k',k}$ is the elliptic projection operator defined by (10).

Lemma 7. *Let $T \in \mathcal{T}_h$ be given and let $\tilde{\mathsf{R}}_{\ell,T}^{k',k}$ be the operator defined by* (12)*. There exists $C > 0$ independent of h_T such that*

$$\left\|\nabla\tilde{\mathsf{R}}_{\ell,T}^{k',k}(\underline{\mathsf{v}}_T)\right\|_{\mathrm{L}^2(T)} \leqslant C\,|\underline{\mathsf{v}}_T|_{\underline{\mathsf{U}}_T^{k',k}} \quad \forall \underline{\mathsf{v}}_T \in \underline{\mathsf{U}}_T^{k',k}\,. \tag{17}$$

Proof. First, we observe that, applying the definition of $\tilde{\mathsf{R}}_{\ell,T}^{k',k}$ in (12),

$$\begin{aligned} \left\|\nabla\tilde{\mathsf{R}}_{\ell,T}^{k',k}(\underline{\mathsf{v}}_T)\right\|_{\mathrm{L}^2(T)}^2 &= \left(\nabla\mathsf{v}_T, \nabla\tilde{\mathsf{R}}_{\ell,T}^{k',k}(\underline{\mathsf{v}}_T)\right)_T \\ &\quad + \left(\mathsf{v}_{\partial T} - \mathsf{v}_T - \mathcal{E}_{\partial T}^{k',k}(\underline{\mathsf{v}}_T), \mathbf{n}\cdot\nabla\tilde{\mathsf{R}}_{\ell,T}^{k',k}(\underline{\mathsf{v}}_T)\right)_{\partial T} \\ &\leqslant \|\nabla\mathsf{v}_T\|_{\mathrm{L}^2(T)} \left\|\nabla\tilde{\mathsf{R}}_{\ell,T}^{k',k}(\underline{\mathsf{v}}_T)\right\|_{\mathrm{L}^2(T)} \\ &\quad + \left(\|\mathsf{v}_{\partial T} - \mathsf{v}_T\|_{\mathrm{L}^2(\partial T)} + \left\|\mathcal{E}_{\partial T}^{k',k}(\underline{\mathsf{v}}_T)\right\|_{\mathrm{L}^2(\partial T)}\right) \\ &\quad \times \left\|\mathbf{n}\cdot\nabla\tilde{\mathsf{R}}_{\ell,T}^{k',k}(\underline{\mathsf{v}}_T)\right\|_{\mathrm{L}^2(\partial T)}\,. \end{aligned} \tag{18}$$

To estimate the term depending on $\mathcal{E}_{\partial T}^{k',k}(\underline{\mathsf{v}}_T)$ we add and subtract suitable integral means in the definition of $\mathcal{E}_{\partial T}^{k',k}(\underline{\mathsf{v}}_T)$ and we apply the continuity of orthogonal projections, discrete trace and Poincaré inequalities and Lemma 4:

$$\begin{aligned}
\left\|\mathcal{E}_{\partial T}^{k',k}(\underline{\mathsf{v}}_T)\right\|_{\mathrm{L}^2(\partial T)} &= \left\|(\pi_{\partial T}^k - I)\left(\mathsf{R}_T^{k',k}(\underline{\mathsf{v}}_T) - \pi_T^0 \mathsf{R}_T^{k',k}(\underline{\mathsf{v}}_T)\right)\right\|_{\mathrm{L}^2(\partial T)} \\
&\leqslant \left\|\mathsf{R}_T^{k',k}(\underline{\mathsf{v}}_T) - \pi_T^0 \mathsf{R}_T^{k',k}(\underline{\mathsf{v}}_T)\right\|_{\mathrm{L}^2(\partial T)} \\
&\leqslant C h_T^{\frac{1}{2}} \left\|\nabla \mathsf{R}_T^{k',k}(\underline{\mathsf{v}}_T)\right\|_{\mathrm{L}^2(T)} \leqslant C h_T^{\frac{1}{2}} \left|\underline{\mathsf{v}}_T\right|_{\underline{\mathsf{U}}_T^{k',k}} \quad \text{if } k' \in \{k-1, k\}\,, \\
\left\|\mathcal{E}_{\partial T}^{k+1,k}(\underline{\mathsf{v}}_T)\right\|_{\mathrm{L}^2(\partial T)} &= \left\|(\pi_{\partial T}^k - I)\left(\mathsf{v}_T - \pi_T^0 \mathsf{v}_T\right)\right\|_{\mathrm{L}^2(\partial T)} \leqslant \left\|\mathsf{v}_T - \pi_T^0 \mathsf{v}_T\right\|_{\mathrm{L}^2(\partial T)} \\
&\leqslant C h_T^{\frac{1}{2}} \left\|\nabla \mathsf{v}_T\right\|_{\mathrm{L}^2(T)} \leqslant C h_T^{\frac{1}{2}} \left|\underline{\mathsf{v}}_T\right|_{\underline{\mathsf{U}}_T^{k+1,k}} \,.
\end{aligned}$$

Moreover, using a discrete trace inequality we obtain

$$\left\|\mathbf{n} \cdot \nabla \tilde{\mathsf{R}}_{\ell,T}^{k',k}(\underline{\mathsf{v}}_T)\right\|_{\mathrm{L}^2(\partial T)} \leqslant C h_T^{-\frac{1}{2}} \left\|\nabla \tilde{\mathsf{R}}_{\ell,T}^{k',k}(\underline{\mathsf{v}}_T)\right\|_{\mathrm{L}^2(T)} \,.$$

Using the above estimates in (18) we get:

$$\begin{aligned}
\left\|\nabla \tilde{\mathsf{R}}_{\ell,T}^{k',k}(\underline{\mathsf{v}}_T)\right\|_{\mathrm{L}^2(T)}^2 &\leqslant \left\|\nabla \mathsf{v}_T\right\|_{\mathrm{L}^2(T)} \left\|\nabla \tilde{\mathsf{R}}_{\ell,T}^{k',k}(\underline{\mathsf{v}}_T)\right\|_{\mathrm{L}^2(T)} \\
&\quad + C\left(h_T^{-\frac{1}{2}} \left\|\mathsf{v}_{\partial T} - \mathsf{v}_T\right\|_{\mathrm{L}^2(\partial T)} + \left|\underline{\mathsf{v}}_T\right|_{\underline{\mathsf{U}}_T^{k',k}}\right) \left\|\nabla \tilde{\mathsf{R}}_{\ell,T}^{k',k}(\underline{\mathsf{v}}_T)\right\|_{\mathrm{L}^2(T)} \\
&\leqslant C \left|\underline{\mathsf{v}}_T\right|_{\underline{\mathsf{U}}_T^{k',k}} \left\|\nabla \tilde{\mathsf{R}}_{\ell,T}^{k',k}(\underline{\mathsf{v}}_T)\right\|_{\mathrm{L}^2(T)} \,,
\end{aligned}$$

which proves (17). □

2.3 Discrete scheme

The operator $\tilde{\mathsf{R}}_{\ell,T}^{k',k}$ defined by (12) is used to define the bilinear form of the proposed discrete scheme for (1). For a given $T \in \mathcal{T}_h$, let $a_T \colon \underline{\mathsf{U}}_T^{k',k} \times \underline{\mathsf{U}}_T^{k',k} \to \mathbb{R}$ be such that

$$a_T\left(\underline{\mathsf{w}}_T, \underline{\mathsf{v}}_T\right) = \left(\nabla \tilde{\mathsf{R}}_{\ell,T}^{k',k}(\underline{\mathsf{w}}_T), \nabla \tilde{\mathsf{R}}_{\ell,T}^{k',k}(\underline{\mathsf{v}}_T)\right)_T \,. \tag{19}$$

Then we define $a_h \colon \underline{\mathsf{U}}_h^{k',k} \times \underline{\mathsf{U}}_h^{k',k} \to \mathbb{R}$ such that, $\forall \underline{\mathsf{w}}_h, \underline{\mathsf{v}}_h \in \underline{\mathsf{U}}_h^{k',k}$,

$$a_h\left(\underline{\mathsf{w}}_h, \underline{\mathsf{v}}_h\right) = \sum_{T \in \mathcal{T}_h} a_T\left(\underline{\mathsf{w}}_T, \underline{\mathsf{v}}_T\right) \,. \tag{20}$$

The discrete scheme reads: chosen $k' \in \{k-1, k, k+1\}$, find $\underline{\mathsf{u}}_h \in \underline{\mathsf{U}}_{h,0}^{k',k}$ such that

$$a_h\left(\underline{\mathsf{u}}_h, \underline{\mathsf{v}}_h\right) = \sum_{T \in \mathcal{T}_h} \left(f, \mathsf{v}_T\right)_T \,, \quad \forall \underline{\mathsf{v}}_h \in \underline{\mathsf{U}}_{h,0}^{k',k} \,. \tag{21}$$

The well-posedness of (21) is an open problem and is discussed numerically in Section 4.1. For the purpose of proceeding with the error analysis, we assume well-posedness through the following conjecture.

Conjecture 1. *Let $T \in \mathcal{T}_h$ and let $\underline{\mathsf{v}}_T \in \underline{\mathsf{U}}_T^{k',k}$, $k' \in \{k-1, k, k+1\}$ be given. Then, there exists a local integer $\ell \geqslant 0$ depending on T such that there is $\alpha_T > 0$ independent of h_T satisfying*

$$\left\|\nabla \tilde{\mathsf{R}}_{\ell,T}^{k',k}(\underline{\mathsf{v}}_T)\right\|_{\mathrm{L}^2(T)}^2 \geqslant \alpha_T \left|\underline{\mathsf{v}}_T\right|_{\underline{\mathsf{U}}_T^{k',k}}^2 \,. \tag{22}$$

Remark 2. By the definition of $\tilde{\mathsf{R}}^{k',k}_{\ell,T}$, Conjecture 1 is subjected to a necessary condition on the local integer $\ell \geqslant 0$ given by $\dim \tilde{\mathbb{P}}^{k',\ell}_d(T) \geqslant \dim \underline{\mathsf{U}}^{k',k}_T$. We recall from Sections 2.1 and 2.2 that

$$\begin{aligned}\dim \tilde{\mathbb{P}}^{k',\ell}_d(T) &= \dim(\mathbb{P}^{k'+2}_d(T)) + \dim(\mathbb{H}^{k'+2+\ell}_d(T) \setminus \mathbb{H}^{k'+2}_d(T))\,,\\ \dim \underline{\mathsf{U}}^{k',k}_T &= \dim(\mathbb{P}^{k'}_d(T)) + \dim(\mathbb{P}^{k}_{d-1}(\mathcal{F}^T))\,.\end{aligned}$$

If we consider $d = 2$, for $t \geqslant 0$ we have

$$\dim(\mathbb{P}^t_2(T)) = \frac{(t+1)(t+2)}{2}\,, \qquad \dim(\mathbb{H}^t_2(T)) = 2t + 1\,,$$

and we get the following necessary condition:

$$2(\ell + k' + 3) - 1 - N^{\partial}_T(k+1) \geqslant 0\,. \tag{23}$$

On the other hand, if $d = 3$, for $t \geqslant 0$ we have

$$\dim(\mathbb{P}^t_3(T)) = \frac{(t+1)(t+2)(t+3)}{6}\,, \qquad \dim(\mathbb{H}^t_3(T)) = (t+1)^2\,,$$

and we get the following necessary condition:

$$(\ell + k' + 3)^2 - N^{\partial}_T \frac{(k+1)(k+2)}{2} \geqslant 0\,. \tag{24}$$

We underline that we always choose $\ell \geqslant 0$ even if the lower bound provided by (23) or (24) is negative.

Employing Lemma 7 we obtain the following well-posedness result subject to Conjecture 1.

Lemma 8. *Let $\underline{\mathsf{w}}_h, \underline{\mathsf{v}}_h \in \underline{\mathsf{U}}^{k',k}_h$ be given. Then, for any choice of ℓ there exists $\omega > 0$ independent of h such that*

$$a_h(\underline{\mathsf{w}}_h, \underline{\mathsf{v}}_h) \leqslant \omega \, \|\underline{\mathsf{w}}_h\|_{\underline{\mathsf{U}}^{k',k}_{h,0}} \|\underline{\mathsf{v}}_h\|_{\underline{\mathsf{U}}^{k',k}_{h,0}}\,. \tag{25}$$

Moreover, if Conjecture 1 is verified, let $\tilde{\mathsf{R}}^{k',k}_{\ell,T}(\underline{\mathsf{w}}_T)$ be built locally on each $T \in \mathcal{T}_h$ such that (22) holds true. Then, there exists $\alpha > 0$ independent of h such that

$$\alpha \, \|\underline{\mathsf{w}}_h\|^2_{\underline{\mathsf{U}}^{k',k}_{h,0}} \leqslant a_h(\underline{\mathsf{w}}_h, \underline{\mathsf{w}}_h)\,, \quad \forall \underline{\mathsf{w}}_h \in \underline{\mathsf{U}}^{k',k}_h\,. \tag{26}$$

Then, (21) has a unique solution.

Proof. Recall that

$$a_h(\underline{\mathsf{w}}_h, \underline{\mathsf{v}}_h) = \sum_{T \in \mathcal{T}_h} \left(\nabla \tilde{\mathsf{R}}^{k',k}_{\ell,T}(\underline{\mathsf{w}}_T), \nabla \tilde{\mathsf{R}}^{k',k}_{\ell,T}(\underline{\mathsf{v}}_T) \right)_T\,.$$

Then (25) follows by applying the Cauchy-Schwarz inequality and Lemma 7. Moreover, (26) follows by applying (22), with $\alpha = \min_{T \in \mathcal{T}_h} \alpha_T$. □

3 A priori error estimates

The a priori error analysis of the new schemes is conducted following [24, Chapter 2], with the aim of showing that the presented schemes exhibit the same convergence behaviors as standard HHO schemes. The approximation results below are used in the error analysis.

Lemma 9. *Let $v \in \mathrm{H}^1(\Omega)$ be such that $\forall T \in \mathcal{T}_h$, $v \in \mathrm{H}^{1+s}(T)$ for some $s \geqslant 0$ and let E_T^{k+1} be defined $\forall T \in \mathcal{T}_h$ by (10). Then, there exists $C > 0$ independent of h_T such that,*

$$\left\|\nabla v - \nabla \mathsf{E}_T^{k+1}(v)\right\|_{\mathrm{L}^2(T)}^2 + h_T^{-2}\left\|v - \mathsf{E}_T^{k+1}(v)\right\|_{\mathrm{L}^2(T)}^2 \leqslant C h_T^{2\min\{s,k+1\}} |v|_{\mathrm{H}^{1+s}(T)}^2 . \tag{27}$$

Moreover, if $\forall T \in \mathcal{T}_h$, $v \in \mathrm{H}^{1+s}(T)$ with $s > \frac{1}{2}$, then there exists $C > 0$ independent of h_T such that,

$$\left\|\nabla\left(v_{|T} - \mathsf{E}_T^{k+1}(v)\right)\right\|_{\mathrm{L}^2(\partial T)}^2 \leqslant C h_T^{2\min\{s,k+1\}-1} |v|_{\mathrm{H}^{1+s}(T)}^2 . \tag{28}$$

Proof. The estimate (27) is a known result in polynomial approximation theory. To prove (28), we recall the following two results from [24, Lemma 2.4 and Lemma 2.5]. For any given polynomial degree $t \in \mathbb{N}$, there exists $C > 0$ independent of h_T such that $\forall T \in \mathcal{T}_h$ and $\forall q \in \mathbb{P}_d^t(T)$

$$\|q\|_{\mathrm{L}^2(\partial T)} \leqslant C h_T^{-\frac{1}{2}} \|q\|_{\mathrm{L}^2(T)} . \tag{29}$$

Moreover, there exists $C > 0$ independent of h_T such that, for any $v \in \mathrm{H}^1(\Omega)$ satisfying $v \in \mathrm{H}^{1+s}(T)$ $\forall T \in \mathcal{T}_h$ for some $s > \frac{1}{2}$, it holds true that

$$\left\|\nabla\left(v_{|T} - \pi_T^{k+1} v\right)\right\|_{\mathrm{L}^2(\partial T)} \leqslant C h_T^{\min\{s,k+1\}-\frac{1}{2}} |v|_{\mathrm{H}^{1+s}(T)} . \tag{30}$$

Hence, applying the triangle inequality, the discrete trace inequality (29), and the bounds (30) and (27), we obtain

$$\begin{aligned}
\left\|\nabla\left(v_{|T} - \mathsf{E}_T^{k+1}(v)\right)\right\|_{\mathrm{L}^2(\partial T)} &\leqslant \left\|\nabla\left(v_{|T} - \pi_T^{k+1} v\right)\right\|_{\mathrm{L}^2(\partial T)} + \left\|\nabla\left(\pi_T^{k+1} v - \mathsf{E}_T^{k+1}(v)\right)\right\|_{\mathrm{L}^2(\partial T)} \\
&\leqslant C h_T^{-\frac{1}{2}} \left(h_T^{\min\{s,k+1\}} |v|_{\mathrm{H}^{1+s}(T)} + \left\|\nabla\left(\pi_T^{k+1} v - \mathsf{E}_T^{k+1}(v)\right)\right\|_{\mathrm{L}^2(T)}\right) \\
&\leqslant C h_T^{-\frac{1}{2}} \left(h_T^{\min\{s,k+1\}} |v|_{\mathrm{H}^{1+s}(T)} + \left\|\nabla\left(\pi_T^{k+1} v - v\right)\right\|_{\mathrm{L}^2(T)}\right. \\
&\qquad \left. + \left\|\nabla\left(v - \mathsf{E}_T^{k+1}(v)\right)\right\|_{\mathrm{L}^2(T)}\right) \\
&\leqslant C h_T^{\min\{s,k+1\}-\frac{1}{2}} |v|_{\mathrm{H}^{1+s}(T)} .
\end{aligned}$$

□

Lemma 10. *Let $u \in \mathrm{H}^1(\Omega)$ be the solution to (1). Assume that $\forall T \in \mathcal{T}_h$, $u \in \mathrm{H}^{1+s}(T)$ for some $s > \frac{1}{2}$. Moreover, assume Conjecture 1 holds true and let $\underline{\mathsf{u}}_h$ be the unique solution to (21), where $\tilde{\mathsf{R}}_{\ell,T}^{k',k}$ is built locally for each $T \in \mathcal{T}_h$ with ℓ satisfying Conjecture 1. Then there exists $C > 0$ independent of the mesh size h such that*

$$\left\|\underline{\mathsf{u}}_h - \underline{\mathsf{I}}_h^{k',k}(u)\right\|_{\underline{\mathsf{U}}_{h,0}^{k',k}} \leqslant C\left(\sum_{T \in \mathcal{T}_h} h_T^{2\min\{s,k+1\}} |u|_{\mathrm{H}^{1+s}(T)}^2\right)^{\frac{1}{2}} . \tag{31}$$

Proof. Let $\underline{\mathsf{e}}_h := \underline{\mathsf{u}}_h - \underline{\mathsf{I}}_h^{k',k}(u)$. Since Conjecture 1 is assumed to be true by hypothesis, applying Lemma 8 and the discrete problem (21) we get

$$\begin{aligned}
\left\|\underline{\mathsf{u}}_h - \underline{\mathsf{I}}_h^{k',k}(u)\right\|_{\underline{\mathsf{U}}_{h,0}^{k',k}}^2 &\leqslant \alpha^{-1} a_h\left(\underline{\mathsf{u}}_h - \underline{\mathsf{I}}_h^{k',k}(u), \underline{\mathsf{e}}_h\right) \\
&= \alpha^{-1}\left|\sum_{T \in \mathcal{T}_h} (f, \mathsf{e}_T)_T - a_T\left(\underline{\mathsf{I}}_T^{k',k}(u), \underline{\mathsf{e}}_T\right)\right| ,
\end{aligned}$$

where $\underline{\mathsf{e}}_T = (\mathsf{e}_T, \mathsf{e}_{\partial T})$, $\mathsf{e}_T = \mathsf{u}_T - \pi_T^{k'} u$ and $\mathsf{e}_{\partial T} = \mathsf{u}_{\partial T} - \pi_{\partial T}^{k} u$. To estimate the above term, we introduce the local elliptic projection $\mathsf{E}_T^{k+1}(u)$, the shorthand notation $e_E = u_{|T} - \mathsf{E}_T^{k+1}(u)$ and by the triangle inequality, we obtain

$$\begin{aligned}\left|\sum_{T\in\mathcal{T}_h} (f, \mathsf{e}_T)_T - a_T\left(\underline{\mathsf{I}}_T^{k',k}(u), \underline{\mathsf{e}}_T\right)\right| &\leqslant \left|\sum_{T\in\mathcal{T}_h} a_T\left(\underline{\mathsf{I}}_T^{k',k}(e_E), \underline{\mathsf{e}}_T\right)\right| \\ &\quad + \left|\sum_{T\in\mathcal{T}_h} (f, \mathsf{e}_T)_T - a_T\left(\underline{\mathsf{I}}_T^{k',k}(\mathsf{E}_T^{k+1}(u)), \underline{\mathsf{e}}_T\right)\right| \\ &=: \tau_1 + \tau_2 \,.\end{aligned} \tag{32}$$

The first term is bounded by the continuity of a_h and $\underline{\mathsf{I}}_T^{k',k}$, given by (25) and (8), respectively, and by the estimate (27):

$$\begin{aligned}\tau_1 = \left|\sum_{T\in\mathcal{T}_h} a_T\left(\underline{\mathsf{I}}_T^{k',k}(e_E), \underline{\mathsf{e}}_T\right)\right| &\leqslant C\left(\sum_{T\in\mathcal{T}_h} \left|\underline{\mathsf{I}}_T^{k',k}(e_E)\right|^2_{\underline{\mathsf{U}}_T^{k',k}}\right)^{\frac{1}{2}} \|\underline{\mathsf{e}}_h\|_{\underline{\mathsf{U}}_{h,0}^{k',k}} \\ &\leqslant C\left(\sum_{T\in\mathcal{T}_h} \|\nabla e_E\|^2_{\mathrm{L}^2(T)}\right)^{\frac{1}{2}} \|\underline{\mathsf{e}}_h\|_{\underline{\mathsf{U}}_{h,0}^{k',k}} \\ &\leqslant C\left(\sum_{T\in\mathcal{T}_h} h_T^{2\min\{s,k+1\}} |u|^2_{\mathrm{H}^{1+s}(T)}\right)^{\frac{1}{2}} \|\underline{\mathsf{e}}_h\|_{\underline{\mathsf{U}}_{h,0}^{k',k}} \,.\end{aligned}$$

To bound the second term in (32), we first observe that (1) implies $f = -\Delta u$ in $\mathrm{L}^2(\Omega)$. Moreover, since $\mathsf{u}_{\partial T}$ is unique on each edge and vanishes on $\partial\Omega$ and $\mathbf{n}\cdot\nabla u \in \mathrm{L}^2(\partial T)$, it holds true that $\sum_{T\in\mathcal{T}_h} (\mathbf{n}\cdot\nabla u, \mathsf{e}_{\partial T})_{\partial T} = 0$. Then,

$$\sum_{T\in\mathcal{T}_h} (f, \mathsf{e}_T)_T = \sum_{T\in\mathcal{T}_h} (-\Delta u, \mathsf{e}_T)_T = \sum_{T\in\mathcal{T}_h} (\nabla u, \nabla \mathsf{e}_T)_T + (\mathbf{n}\cdot\nabla u, \mathsf{e}_{\partial T} - \mathsf{e}_T)_{\partial T} \,. \tag{33}$$

Moreover, if we apply Lemma 5 and Lemma 6, the definition of $\mathsf{R}_T^{k',k}(\underline{\mathsf{v}}_T)$ (9) and the definition of E_T^{k+1} (10), we get

$$\begin{aligned}a_T\left(\underline{\mathsf{I}}_T^{k',k}(\mathsf{E}_T^{k+1}(u)), \underline{\mathsf{e}}_T\right) &= \left(\nabla\tilde{\mathsf{R}}_{\ell,T}^{k',k}(\underline{\mathsf{I}}_T^{k',k}(\mathsf{E}_T^{k+1}(u))), \nabla\tilde{\mathsf{R}}_{\ell,T}^{k',k}(\underline{\mathsf{e}}_T)\right)_T \\ &= \left(\nabla\mathsf{E}_T^{k+1}(u), \nabla\mathsf{R}_T^{k',k}(\underline{\mathsf{e}}_T)\right)_T \\ &= \left(\nabla\mathsf{E}_T^{k+1}(u), \nabla\mathsf{e}_T\right)_T - \left(\mathbf{n}\cdot\nabla\mathsf{E}_T^{k+1}(u), \mathsf{e}_{\partial T} - \mathsf{e}_T\right)_{\partial T} \\ &= (\nabla u, \nabla\mathsf{e}_T)_T - \left(\mathbf{n}\cdot\nabla\mathsf{E}_T^{k+1}(u), \mathsf{e}_{\partial T} - \mathsf{e}_T\right)_{\partial T} \,.\end{aligned} \tag{34}$$

The next estimate follows applying (33) and (34) in the first line and the bound is concluded by using the approximation property of E_T^{k+1} in (28):

$$\begin{aligned}
\tau_2 &= \left| \sum_{T\in\mathcal{T}_h} (f, \mathsf{e}_T)_T - a_T\left(\underline{\mathsf{I}}_T^{k',k}(\mathsf{E}_T^{k+1}(u)), \underline{\mathsf{e}}_T\right) \right| = \left| \sum_{T\in\mathcal{T}_h} (\mathbf{n}\cdot\nabla e_E, \mathsf{e}_{\partial T} - \mathsf{e}_T)_{\partial T} \right| \\
&\leqslant \sum_{T\in\mathcal{T}_h} \|\mathbf{n}\cdot\nabla e_E\|_{\mathrm{L}^2(\partial T)} \|\mathsf{e}_{\partial T} - \mathsf{e}_T\|_{\mathrm{L}^2(\partial T)} \\
&\leqslant C \left(\sum_{T\in\mathcal{T}_h} h_T \|\nabla e_E\|^2_{\mathrm{L}^2(\partial T)} \right)^{\frac{1}{2}} \left(\sum_{T\in\mathcal{T}_h} h_T^{-1} \|\mathsf{e}_{\partial T} - \mathsf{e}_T\|^2_{\mathrm{L}^2(\partial T)} \right)^{\frac{1}{2}} \\
&\leqslant C \left(\sum_{T\in\mathcal{T}_h} h_T^{2\min\{s,k+1\}} |u|^2_{\mathrm{H}^{1+s}(T)} \right)^{\frac{1}{2}} \|\underline{\mathsf{e}}_h\|_{\underline{\mathsf{U}}_{h,0}^{k',k}} .
\end{aligned}$$

□

Theorem 1. *Let $u \in \mathrm{H}^1(\Omega)$ be the solution to (1). Assume that $\forall T \in \mathcal{T}_h$, $u \in \mathrm{H}^{1+s}(T)$ for some $s > \frac{1}{2}$. Moreover, assume Conjecture 1 holds true and let $\underline{\mathsf{u}}_h \in \underline{\mathsf{U}}_{h,0}^{k',k}$ be the unique solution to (21), where $\tilde{\mathsf{R}}_{\ell,T}^{k',k}$ is built locally for each $T \in \mathcal{T}_h$ with ℓ satisfying Conjecture 1. Then there exists $C > 0$ independent of the mesh size h such that*

$$\left(\sum_{T\in\mathcal{T}_h} \left\| \nabla u - \nabla \mathsf{R}_T^{k',k}(\underline{\mathsf{u}}_T) \right\|^2_{\mathrm{L}^2(T)} \right)^{\frac{1}{2}} \leqslant C \left(\sum_{T\in\mathcal{T}_h} h_T^{2\min\{s,k+1\}} |u|^2_{\mathrm{H}^{1+s}(T)} \right)^{\frac{1}{2}} .$$

Proof. Adding and subtracting the operator $\mathsf{E}_T^{k+1} = \mathsf{R}_T^{k',k} \circ \underline{\mathsf{I}}_T^{k',k}$, using a triangle inequality and Lemma 4 we get, for any $T \in \mathcal{T}_h$,

$$\begin{aligned}
\left\| \nabla u - \nabla \mathsf{R}_T^{k',k}(\underline{\mathsf{u}}_T) \right\|_{\mathrm{L}^2(T)} &\leqslant \left\| \nabla u - \nabla \mathsf{E}_T^{k+1}(u) \right\|_{\mathrm{L}^2(T)} + \left\| \nabla \mathsf{R}_T^{k',k}\left(\underline{\mathsf{u}}_T - \underline{\mathsf{I}}_T^{k',k}(u) \right) \right\|_{\mathrm{L}^2(T)} \\
&\leqslant \left\| \nabla u - \nabla \mathsf{E}_T^{k+1}(u) \right\|_{\mathrm{L}^2(T)} + C \left| \underline{\mathsf{u}}_T - \underline{\mathsf{I}}_T^{k',k}(u) \right|_{\underline{\mathsf{U}}_T^{k',k}} .
\end{aligned}$$

The thesis is then obtained summing over $T \in \mathcal{T}_h$, bounding the first term using Lemma 9 and the second term using Lemma 10. □

Remark 3. If $s \geqslant k+1$ the error estimate in Theorem 1 is of the optimal order $O(h^{k+1})$.

Remark 4. The regularity assumptions in Lemma 10 and Theorem 1 have been done for simplicity, following the approach in [24]. Indeed, this is the minimum regularity that yields $\mathbf{n}\cdot\nabla u \in \mathrm{L}^2(\partial T)$. Recently [34], a refined functional setting has been defined to extend the analysis to $u \in \mathrm{H}^{1+s}(\Omega)$ with $s > 0$.

To get an L^2-error estimate, let $r \in \left(\frac{1}{2}, 1\right]$ denote the real number such that, for any given $g \in \mathrm{L}^2(\Omega)$ there exists $\psi \in \mathrm{H}^{1+r}(\Omega) \cap \mathrm{H}^1_0(\Omega)$ solving the dual problem

$$(\nabla v, \nabla \psi)_\Omega = (v, g)_\Omega , \quad \forall v \in \mathrm{H}^1_0(\Omega) . \tag{35}$$

Notice that r depends on the geometry of Ω [36] and if Ω is convex we get $r = 1$. By elliptic regularity, ψ satisfies the estimate

$$\|\psi\|_{\mathrm{H}^{1+r}(\Omega)} \leqslant C \|g\|_{\mathrm{L}^2(\Omega)} . \tag{36}$$

Lemma 11. *Let $u \in \mathrm{H}^1_0(\Omega)$ be the solution to (1). Assume that $\forall T \in \mathcal{T}_h$, $u \in \mathrm{H}^{1+s}(T)$ and $f \in \mathrm{H}^t(T)$ for some $s > \frac{1}{2}$, $t \geqslant 0$. Moreover, assume Conjecture 1 holds true and let $\underline{\mathsf{u}}_h \in \underline{\mathsf{U}}_{h,0}^{k',k}$ be the unique solution to*

(21), *where* $\tilde{\mathsf{R}}^{k',k}_{\ell,T}$ *is built locally for each* $T \in \mathcal{T}_h$ *with* ℓ *satisfying Conjecture 1. Then there exists* $C > 0$ *independent of the mesh size* h *such that*

$$\left(\sum_{T\in\mathcal{T}_h} \left\|\mathsf{u}_T - \pi^{k'}_T u\right\|^2_{\mathrm{L}^2(T)}\right)^{\frac{1}{2}} \leqslant Ch^r \left(\left(\sum_{T\in\mathcal{T}_h} h_T^{2\min\{s,k+1\}} |u|^2_{\mathrm{H}^{1+s}(T)}\right)^{\frac{1}{2}} + \left(\sum_{T\in\mathcal{T}_h} h_T^{2(\min\{t,k'+1\}+1+\min\{r,k'\}-r)} |f|^2_{\mathrm{H}^t(T)}\right)^{\frac{1}{2}}\right) \quad (37)$$

where r *is the real number such that* (35) *and* (36) *hold true.*

Proof. Let $e_h \in \mathrm{L}^2(\Omega)$ be such that $e_T := e_h|_T = \mathsf{u}_T - \pi^{k'}_T u \in \mathbb{P}^{k'}_d(T)$ for all $T \in \mathcal{T}_h$. Let $\psi \in \mathrm{H}^{1+r}(\Omega) \cap \mathrm{H}^1_0(\Omega)$ with $r \in \left(\frac{1}{2}, 1\right]$ be such that

$$(\nabla v, \nabla\psi)_\Omega = (v, e_h)_\Omega \quad \forall v \in \mathrm{H}^1_0(\Omega) \ ,$$

hence $e_h = -\Delta\psi$ in $\mathrm{L}^2(\Omega)$. Then, $\forall T \in \mathcal{T}_h$ let $e_{\partial T} \in \mathrm{L}^2(\partial T)$ be such that $\forall F \in \mathcal{F}^T$, $e_{\partial T}|_F = \mathsf{u}_{\partial T} - \pi^k_{\partial T}(u)|_F \in \mathrm{H}^{\frac{1}{2}}(F)$. Since $\sum_{T\in\mathcal{T}_h} (e_{\partial T}, \mathbf{n}\cdot\nabla\psi)_{\partial T} = 0$, and by introducing the elliptic projection E^{k+1}_T locally, we infer that

$$\begin{aligned}\|e_h\|^2_{\mathrm{L}^2(\Omega)} &= -(e_h, \Delta\psi)_\Omega = \sum_{T\in\mathcal{T}_h} (\nabla e_T, \nabla\psi)_T + (e_{\partial T} - e_T, \mathbf{n}\cdot\nabla\psi)_{\partial T} \\ &= \sum_{T\in\mathcal{T}_h} \left(\nabla e_T, \nabla\mathsf{E}^{k+1}_T(\psi)\right)_T + \left(e_{\partial T} - e_T, \mathbf{n}\cdot\nabla\mathsf{E}^{k+1}_T(\psi)\right)_{\partial T} \\ &\quad + \left(e_{\partial T} - e_T, \mathbf{n}\cdot\nabla(\psi - \mathsf{E}^{k+1}_T(\psi))\right)_{\partial T} .\end{aligned} \quad (38)$$

Let us call τ_1 the sum of the two first terms on the right hand side of (38) and τ_2 the rightmost one. To bound τ_1, we first recall that since $\mathsf{E}^{k+1}_T(\psi) \in \mathbb{P}^{k+1}_d(T)$, then $\left(\mathcal{E}^{k',k}_{\partial T}\left(\underline{\mathsf{u}}_T - \underline{\mathsf{I}}^{k',k}_T(u)\right), \mathbf{n}\cdot\nabla\mathsf{E}^{k+1}_T(\psi)\right)_{\partial T} = 0$. Hence, this identity along with the definition of $\tilde{\mathsf{R}}^{k',k}_{\ell,T}$ (12) leads to

$$\begin{aligned}\tau_1 &= \sum_{T\in\mathcal{T}_h} \left(\nabla e_T, \nabla\mathsf{E}^{k+1}_T(\psi)\right)_T + \left(e_{\partial T} - e_T, \mathbf{n}\cdot\nabla\mathsf{E}^{k+1}_T(\psi)\right)_{\partial T} \\ &= \sum_{T\in\mathcal{T}_h} \left(\nabla\tilde{\mathsf{R}}^{k',k}_{\ell,T}(\underline{\mathsf{u}}_T - \underline{\mathsf{I}}^{k',k}_T(u)), \nabla\mathsf{E}^{k+1}_T(\psi)\right)_T \\ &= \sum_{T\in\mathcal{T}_h} \left(\nabla\tilde{\mathsf{R}}^{k',k}_{\ell,T}\left(\underline{\mathsf{u}}_T - \underline{\mathsf{I}}^{k',k}_T(u)\right), \nabla\mathsf{E}^{k+1}_T(\psi) - \nabla\tilde{\mathsf{R}}^{k',k}_{\ell,T}\left(\underline{\mathsf{I}}^{k',k}_T(\psi)\right)\right)_T \\ &\quad + a_h\left(\underline{\mathsf{u}}_h - \underline{\mathsf{I}}^{k',k}_h(u), \underline{\mathsf{I}}^{k',k}_h(\psi)\right) := \tau_{1,1} + \tau_{1,2} .\end{aligned} \quad (39)$$

$\tau_{1,1}$ is bounded exploiting Lemma 5, the Cauchy-Schwarz inequality, the continuity of $\tilde{\mathsf{R}}^{k',k}_{\ell,T}$ (17) and $\underline{\mathsf{I}}^{k',k}_T$

(8), Lemma 9 and Lemma 10 and the elliptic regularity property (36):

$$\begin{aligned}
\tau_{1,1} &= \sum_{T\in\mathcal{T}_h} \left(\nabla\tilde{\mathsf{R}}^{k',k}_{\ell,T}\left(\underline{\mathsf{u}}_T - \underline{\mathsf{I}}^{k',k}_T(u)\right), \nabla\mathsf{E}^{k+1}_T(\psi) - \nabla\tilde{\mathsf{R}}^{k',k}_{\ell,T}\left(\underline{\mathsf{I}}^{k',k}_T(\psi)\right)\right)_T \\
&= \sum_{T\in\mathcal{T}_h} \left(\nabla\tilde{\mathsf{R}}^{k',k}_{\ell,T}\left(\underline{\mathsf{u}}_T - \underline{\mathsf{I}}^{k',k}_T(u)\right), \nabla\tilde{\mathsf{R}}^{k',k}_{\ell,T}\left(\underline{\mathsf{I}}^{k',k}_T(\mathsf{E}^{k+1}_T(\psi)-\psi)\right)\right)_T \\
&\leqslant \sum_{T\in\mathcal{T}_h} \left\|\nabla\tilde{\mathsf{R}}^{k',k}_{\ell,T}\left(\underline{\mathsf{u}}_T - \underline{\mathsf{I}}^{k',k}_T(u)\right)\right\|_{\mathrm{L}^2(T)} \left\|\nabla\tilde{\mathsf{R}}^{k',k}_{\ell,T}\left(\underline{\mathsf{I}}^{k',k}_T(\mathsf{E}^{k+1}_T(\psi)-\psi)\right)\right\|_{\mathrm{L}^2(T)} \\
&\leqslant C\left\|\underline{\mathsf{u}}_h - \underline{\mathsf{I}}^{k',k}_h(u)\right\|_{\underline{\mathsf{U}}^{k',k}_{h,0}} \left(\sum_{T\in\mathcal{T}_h}\left\|\nabla\psi - \nabla\mathsf{E}^{k+1}_T(\psi)\right\|^2_{\mathrm{L}^2(T)}\right)^{\frac12} \\
&\leqslant Ch^r\left(\sum_{T\in\mathcal{T}_h} h_T^{2\min\{s,k+1\}}\,|u|^2_{\mathrm{H}^{1+s}(T)}\right)^{\frac12}\|\psi\|_{\mathrm{H}^{1+r}(\Omega)} \\
&\leqslant Ch^r\left(\sum_{T\in\mathcal{T}_h} h_T^{2\min\{s,k+1\}}\,|u|^2_{\mathrm{H}^{1+s}(T)}\right)^{\frac12}\|e_h\|_{\mathrm{L}^2(\Omega)}\,.
\end{aligned}$$

The second term in (39) can be rewritten exploiting the fact that $\underline{\mathsf{u}}_h$ solves (21) and u solves (1), as follows:

$$\begin{aligned}
\tau_{1,2} = a_h\left(\underline{\mathsf{u}}_h - \underline{\mathsf{I}}^{k',k}_h(u), \underline{\mathsf{I}}^{k',k}_h(\psi)\right) &= \sum_{T\in\mathcal{T}_h}\left(f, \pi^{k'}_T\psi - \psi\right)_T + (\nabla u,\nabla\psi)_\Omega \\
- a_h\left(\underline{\mathsf{I}}^{k',k}_h(u), \underline{\mathsf{I}}^{k',k}_h(\psi)\right) &= \tau_{1,2,1} + \tau_{1,2,2} + \tau_{1,2,3}\,.
\end{aligned} \tag{40}$$

The first term in (40) is bounded by the Cauchy-Schwarz inequality and exploiting the approximation properties of $\pi^{k'}_T$ and (36):

$$\begin{aligned}
\tau_{1,2,1} &= \sum_{T\in\mathcal{T}_h}\left(f - \pi^{k'}_T f, \pi^{k'}_T\psi - \psi\right)_T \leqslant \sum_{T\in\mathcal{T}_h}\left\|f - \pi^{k'}_T f\right\|_{\mathrm{L}^2(T)}\left\|\pi^{k'}_T\psi - \psi\right\|_{\mathrm{L}^2(T)} \\
&\leqslant C\sum_{T\in\mathcal{T}_h} h_T^{\min\{t,k'+1\}}\,|f|_{\mathrm{H}^t(T)}\,h_T^{1+\min\{r,k'\}}\,|\psi|_{\mathrm{H}^{1+r}(T)} \\
&\leqslant Ch^r\left(\sum_{T\in\mathcal{T}_h} h_T^{2(\min\{t,k'+1\}+1+\min\{r,k'\}-r)}\,|f|^2_{\mathrm{H}^t(T)}\right)^{\frac12}\|e_h\|_{\mathrm{L}^2(\Omega)}\,.
\end{aligned}$$

The second and third terms in (40) are rewritten together exploiting (16) and (10), as follows:

$$\begin{aligned}
\tau_{1,2,2} + \tau_{1,2,3} &= \sum_{T\in\mathcal{T}_h}(\nabla u,\nabla\psi)_T - \left(\nabla\tilde{\mathsf{R}}^{k',k}_{\ell,T}(\underline{\mathsf{I}}^{k',k}_T(u)), \nabla\tilde{\mathsf{R}}^{k',k}_{\ell,T}(\underline{\mathsf{I}}^{k',k}_T(\psi))\right)_T \\
&= \sum_{T\in\mathcal{T}_h}\left(\nabla u, \nabla\left(\psi - \mathsf{E}^{k+1}_T(\psi)\right)\right)_T \\
&\quad + \left(\nabla\tilde{\mathsf{R}}^{k',k}_{\ell,T}(\underline{\mathsf{I}}^{k',k}_T(u)), \nabla\left(\mathsf{E}^{k+1}_T(\psi) - \tilde{\mathsf{R}}^{k',k}_{\ell,T}(\underline{\mathsf{I}}^{k',k}_T(\psi))\right)\right)_T \\
&= \sum_{T\in\mathcal{T}_h}\left(\nabla\left(u - \mathsf{E}^{k+1}_T(u)\right), \nabla\left(\psi - \mathsf{E}^{k+1}_T(\psi)\right)\right)_T \\
&\quad + \left(\nabla\left(\tilde{\mathsf{R}}^{k',k}_{\ell,T}(\underline{\mathsf{I}}^{k',k}_T(u)) - \mathsf{E}^{k+1}_T(u)\right), \nabla\left(\mathsf{E}^{k+1}_T(\psi) - \tilde{\mathsf{R}}^{k',k}_{\ell,T}(\underline{\mathsf{I}}^{k',k}_T(\psi))\right)\right)_T\,.
\end{aligned}$$

Hence, we have the following bound owing to the Cauchy-Schwarz inequality, (17), (8), Lemma 9 and (36),

$$
\begin{aligned}
\tau_{1,2,2}+\tau_{1,2,3} &\leqslant \sum_{T\in\mathcal{T}_h} \left\|\nabla\left(u-\mathsf{E}_T^{k+1}(u)\right)\right\|_{\mathrm{L}^2(T)} \left\|\nabla\left(\psi-\mathsf{E}_T^{k+1}(\psi)\right)\right\|_{\mathrm{L}^2(T)} \\
&\quad + \left\|\nabla\tilde{\mathsf{R}}_{\ell,T}^{k',k}\left(\underline{\mathsf{I}}_T^{k',k}(u-\mathsf{E}_T^{k+1}(u))\right)\right\|_{\mathrm{L}^2(T)} \left\|\nabla\tilde{\mathsf{R}}_{\ell,T}^{k',k}\left(\underline{\mathsf{I}}_T^{k',k}(\psi-\mathsf{E}_T^{k+1}(\psi))\right)\right\|_{\mathrm{L}^2(T)} \\
&\leqslant C\left(\sum_{T\in\mathcal{T}_h}\left\|\nabla\left(u-\mathsf{E}_T^{k+1}(u)\right)\right\|_{\mathrm{L}^2(T)}^2\right)^{\frac{1}{2}}\left(\sum_{T\in\mathcal{T}_h}\left\|\nabla\left(\psi-\mathsf{E}_T^{k+1}(\psi)\right)\right\|_{\mathrm{L}^2(T)}^2\right)^{\frac{1}{2}} \\
&\leqslant Ch^r\left(\sum_{T\in\mathcal{T}_h} h_T^{2\min\{s,k+1\}}\,|u|_{\mathrm{H}^{1+s}(T)}^2\right)^{\frac{1}{2}}\|e_h\|_{\mathrm{L}^2(\Omega)} .
\end{aligned}
$$

Finally, going back to (38), τ_2 can be bounded by a trace inequality, Lemma 9, Lemma 10 and (36):

$$
\begin{aligned}
\tau_2 &= \left(e_{\partial T}-e_T,\mathbf{n}\cdot\nabla(\psi-\mathsf{E}_T^{k+1}(\psi))\right)_{\partial T} \\
&\leqslant \|e_{\partial T}-e_T\|_{\mathrm{L}^2(\partial T)}\left\|\mathbf{n}\cdot\nabla(\psi-\mathsf{E}_T^{k+1}(\psi))\right\|_{\mathrm{L}^2(\partial T)} \\
&\leqslant C\left(\sum_{T\in\mathcal{T}_h} h_T^{-1}\|\mathsf{e}_{\partial T}-\mathsf{e}_T\|_{\mathrm{L}^2(\partial T)}^2\right)^{\frac{1}{2}} \\
&\quad\times\left(\sum_{T\in\mathcal{T}_h}\left\|\nabla\psi-\nabla\mathsf{E}_T^{k+1}(\psi)\right\|_{\mathrm{L}^2(T)}^2+h_T^{-2}\left\|\psi-\mathsf{E}_T^{k+1}(\psi)\right\|_{\mathrm{L}^2(T)}^2\right)^{\frac{1}{2}} \\
&\leqslant C\left\|\underline{\mathsf{u}}_h-\underline{\mathsf{I}}_h^{k',k}(u)\right\|_{\underline{\mathsf{U}}_{h,0}^{k',k}} h^r\|\psi\|_{\mathrm{H}^{1+r}(\Omega)} \\
&\leqslant Ch^r\left(\sum_{T\in\mathcal{T}_h} h_T^{2\min\{s,k+1\}}\,|u|_{\mathrm{H}^{1+s}(T)}^2\right)^{\frac{1}{2}}\|e_h\|_{\mathrm{L}^2(\Omega)} .
\end{aligned}
$$

□

Theorem 2. *Let $u\in\mathrm{H}_0^1(\Omega)$ be the solution to* (1)*. Assume that $\forall T\in\mathcal{T}_h$, $u\in\mathrm{H}^{1+s}(T)$ and $f\in\mathrm{H}^t(T)$ for some $s>\frac{1}{2}$, $t\geqslant 0$. Moreover, assume Conjecture 1 holds true and let $\underline{\mathsf{u}}_h\in\underline{\mathsf{U}}_{h,0}^{k',k}$ be the unique solution to* (21)*, where $\tilde{\mathsf{R}}_{\ell,T}^{k',k}$ is built locally for each $T\in\mathcal{T}_h$ with ℓ satisfying Conjecture 1. Then there exists $C>0$ independent of the mesh size h such that*

$$
\begin{aligned}
\left(\sum_{T\in\mathcal{T}_h}\left\|u-\mathsf{R}_T^{k',k}(\underline{\mathsf{u}}_T)\right\|_{\mathrm{L}^2(T)}^2\right)^{\frac{1}{2}} \leqslant Ch^r\Bigg(&\left(\sum_{T\in\mathcal{T}_h} h_T^{2\min\{s,k+1\}}\,|u|_{\mathrm{H}^{1+s}(T)}^2\right)^{\frac{1}{2}} \\
&+\left(\sum_{T\in\mathcal{T}_h} h_T^{2(\min\{t,k'+1\}+1+\min\{r,k'\}-r)}\,|f|_{\mathrm{H}^t(T)}^2\right)^{\frac{1}{2}}\Bigg), \quad (41)
\end{aligned}
$$

where r is the real number such that (35) *and* (36) *hold true.*

Proof. In the following, we assume for simplicity that $h_T\leqslant 1$ $\forall T\in\mathcal{T}_h$, so that $h_T\leqslant h_T^r$ $\forall T\in\mathcal{T}_h$. Adding and subtracting the operator $\mathsf{E}_T^{k+1}=\mathsf{R}_T^{k',k}\circ\underline{\mathsf{I}}_T^{k',k}$, using a triangle inequality we get, for any $T\in\mathcal{T}_h$,

$$
\left\|u-\mathsf{R}_T^{k',k}(\underline{\mathsf{u}}_T)\right\|_{\mathrm{L}^2(T)} \leqslant \left\|u-\mathsf{E}_T^{k+1}(u)\right\|_{\mathrm{L}^2(T)}+\left\|\mathsf{R}_T^{k',k}\left(\underline{\mathsf{u}}_T-\underline{\mathsf{I}}_T^{k',k}(u)\right)\right\|_{\mathrm{L}^2(T)} .
$$

The first term is bounded using (27), obtaining (41) since $r \leqslant 1$ when $h_T \leqslant 1$. To bound the second term, we resort to a Poincaré-Friedrichs inequality and exploit (11), the second condition in (9) and the continuity of the integral mean operator:

$$\begin{aligned}\left\|\mathsf{R}_T^{k',k}\left(\underline{\mathsf{u}}_T - \underline{\mathsf{I}}_T^{k',k}(u)\right)\right\|_{\mathrm{L}^2(T)} &\leqslant Ch_T\left(\left\|\nabla\mathsf{R}_T^{k',k}\left(\underline{\mathsf{u}}_T - \underline{\mathsf{I}}_T^{k',k}(u)\right)\right\|_{\mathrm{L}^2(T)}\right.\\ &\qquad\left.+\left|\frac{1}{|T|}\int_T \mathsf{R}_T^{k',k}\left(\underline{\mathsf{u}}_T - \underline{\mathsf{I}}_T^{k',k}(u)\right)\right|\right)\\ &\leqslant C\left(h_T\left|\underline{\mathsf{u}}_T - \underline{\mathsf{I}}_T^{k',k}(u)\right|_{\underline{\mathsf{U}}_T^{k',k}} + \left\|\mathsf{u}_T - \pi_T^{k'}u\right\|_{\mathrm{L}^2(T)}\right).\end{aligned}$$

Thus the estimate (41) follows applying the estimates (31) and (37). □

Remark 5. The estimate in Theorem 2 is of the optimal order $O(h^{k+2})$ if Ω is convex ($r = 1$), $s \geqslant k+1$, $\min\{t, k'+1\} \geqslant k$ and $k' \geqslant 1$. In particular, when Ω is convex, $s \geqslant k+1$ and $k' \geqslant 1$, the optimal order is achieved if $f \in \mathrm{H}^{s-1}(\Omega)$. For the HHO(0,0) scheme, the optimal order $O(h^2)$ is achieved when Ω is convex, $u \in \mathrm{H}^2(T)$ and $f \in \mathrm{H}^1(T)$ for all $T \in \mathcal{T}_h$. For the HHO(0,1) scheme, the best we can get is a sub-optimal order of convergence $O(h^2)$, obtained assuming a convex Ω, $u \in \mathrm{H}^3(T)$ and $f \in \mathrm{H}^2(T)$. This sub-optimality is a known result in HHO theory [24].

4 Numerical results

In this section we study numerically the proposed method from two different points of view. First, we evaluate the local numerical coercivity on different sets of polytopes, to determine the minimum ℓ required for local coercivity starting from the necessary conditions given in Remark (2). Afterwards, we verify the rates of convergence of the proposed methods on a variety of 2D and 3D meshes. The proposed numerical method was implemented in the open-source DiSk++ numerical library (`https://github.com/wareHHOuse/diskpp`) [21], which allows fast prototyping of discontinuous methods for PDEs.

4.1 Numerical coercivity tests

For each polytope T considered in this section, we compute the local stiffness matrices $\mathbf{S}_{a_T}$ corresponding to the bilinear form a_T defined by (19). Elemental matrices are built choosing suitable bases for the polynomial spaces involved, employing the scaled monomials described in [20]. We also remark, that in order to evaluate the face-based polynomials, an affine geometric transformation $\mathbf{T}_F : \mathbb{R}^{d-1} \to H_F$, where H_F is the affine hyperplane in $\mathbb{R}^d$ supporting F, is needed. Therefore,

$$\mathbb{P}_{d-1}^k(F) := \mathbb{P}_{d-1}^k \circ (\mathbf{T}_F^{-1})_{|F}.$$

For each matrix $\mathbf{S}_{a_T}$, we compute the $\left(N_T^{k',k} - 1\right)$-largest eigenvalue σ_T, $N_T^{k',k}$ being the number of local degrees of freedom, see (2). In 2D, for each σ_T we check if it is well detached from zero, ensuring that the rank of the matrix is equal to $N_T^{k',k} - 1$, which is the desired local rank to obtain a globally positive definite linear system. In 3D the same check is done on the quantity σ_T/h_T, as in this case the stiffness matrix scales as h_T.

The analysis above is performed for $k \in \{0,1,2\}$ and for the three possible schemes HHO($k-1,k$), HHO(k,k) and HHO($k+1,k$), looking for the smallest value of ℓ inducing numerical coercivity. In each case, we first set ℓ to be equal to the smallest non-negative value satisfying the necessary condition prescribed by Remark 2, i.e. satisfying (23) in the 2D case and (24) in the 3D case. If numerical coercivity is not verified using this initial guess, we increase ℓ until the rank of $\mathbf{S}_{a_T}$ equals $N_T^{k',k} - 1$. We observe that, even if the value of ℓ given by the necessary condition is also numerically sufficient to obtain the desired rank, the dimension of the reconstruction space may be greater than the dimension of the local HHO space.

Table 1: Values of σ_T computed with HHO$(k-1,k)$ on regular polygons. In parentheses, the value of ℓ.

k	$N_T^\partial = 3$	$N_T^\partial = 4$	$N_T^\partial = 5$	$N_T^\partial = 6$	$N_T^\partial = 7$
1	5.30e-01 (1)	6.67e-01 (2)	7.10e-01 (3)	6.90e-01 (4)	6.56e-01 (5)
2	3.05e-01 (1)	4.09e-01 (3)	3.65e-01 (4)	3.80e-01 (6)	3.20e-01 (7)
k	$N_T^\partial = 8$	$N_T^\partial = 9$	$N_T^\partial = 10$	$N_T^\partial = 11$	$N_T^\partial = 12$
1	6.17e-01 (6)	5.78e-01 (7)	5.40e-01 (8)	5.06e-01 (9)	4.74e-01 (10)
2	3.36e-01 (9)	2.82e-01 (10)	3.02e-01 (12)	2.61e-01 (13)	2.79e-01 (15)
k	$N_T^\partial = 13$	$N_T^\partial = 14$	$N_T^\partial = 15$	$N_T^\partial = 16$	$N_T^\partial = 17$
1	4.45e-01 (11)	4.19e-01 (12)	3.95e-01 (13)	3.73e-01 (14)	3.54e-01 (15)
2	2.46e-01 (16)	2.63e-01 (18)	2.36e-01 (19)	2.51e-01 (21)	2.28e-01 (22)

Table 2: Values of σ_T computed with HHO(k,k) on regular polygons. In parentheses, the value of ℓ.

k	$N_T^\partial = 3$	$N_T^\partial = 4$	$N_T^\partial = 5$	$N_T^\partial = 6$	$N_T^\partial = 7$
0	3.46e+00 (0)	2.00e+00 (0)	1.45e+00 (0)	1.15e+00 (1)	9.63e-01 (1)
1	3.94e-01 (0)	5.23e-01 (1)	5.75e-01 (2)	5.59e-01 (3)	5.45e-01 (4)
2	2.55e-01 (0)	3.00e-01 (2)	3.40e-01 (3)	3.58e-01 (5)	3.20e-01 (6)
k	$N_T^\partial = 8$	$N_T^\partial = 9$	$N_T^\partial = 10$	$N_T^\partial = 11$	$N_T^\partial = 12$
0	8.28e-01 (2)	7.28e-01 (2)	6.50e-01 (3)	5.87e-01 (3)	5.36e-01 (4)
1	5.14e-01 (5)	4.89e-01 (6)	4.60e-01 (7)	4.36e-01 (8)	4.11e-01 (9)
2	3.36e-01 (8)	2.82e-01 (9)	3.02e-01 (11)	2.61e-01 (12)	2.79e-01 (14)
k	$N_T^\partial = 13$	$N_T^\partial = 14$	$N_T^\partial = 15$	$N_T^\partial = 16$	$N_T^\partial = 17$
0	4.93e-01 (4)	4.56e-01 (5)	4.25e-01 (5)	3.98e-01 (6)	3.74e-01 (6)
1	3.90e-01 (10)	3.69e-01 (11)	3.51e-01 (12)	3.33e-01 (13)	3.18e-01 (14)
2	2.46e-01 (15)	2.63e-01 (17)	2.36e-01 (18)	2.51e-01 (20)	2.28e-01 (21)

4.1.1 Regular polygons

Let us consider a set of regular polygons of n vertices, obtained as the convex hull of the set of points $\left\{\left(\cos\left(\frac{2\pi i}{n}\right), \sin\left(\frac{2\pi i}{n}\right)\right) \mid 0 \leqslant i < n\right\}$. In Tables 1, 2 and 3 we report the values of σ_T and, in parentheses, the chosen value of ℓ. We observe that the necessary condition on ℓ given by (23) is numerically sufficient for all the methods and all the polygons. Moreover, the computed values of σ_T are well detached from zero.

4.1.2 Concave polygons

In Table 4 we depict a set of concave polygons and we report in Tables 5, 6 and 7 the computed values of σ_T for each one of the three proposed methods. In parentheses, we report the incremental polynomial degree ℓ, given by (23), observing that in each case analyzed we obtain the numerical stability applying the necessary condition on ℓ. Although, some relatively small values of σ_T are reported, we found that a small increase of ℓ above the necessary condition further detaches σ_T from zero. Let us give more quantitative results taking as examples the two worst cases, happening for $k = 2$ and reported in Table 7. In the first case with $N_T^\partial = 4$, we found that choosing $\ell \in \{2, 3, 4, 5\}$ we get the following increased values of σ_T: 2.10e-04, 1.05e-02, 1.24e-02, 1.39e-02. In the second case with $N_T^\partial = 11$, we found that a progressive enrichment of the basis with $\ell \in \{11, 12, 13, 14\}$ leads to the following increased values of σ_T: 1.45e-10, 7.74e-06, 2.25e-05, 6.50e-05. Thus, the choice of ℓ might result from a reasonable compromise of an improved numerical stability and computational cost. We observe that each increase of ℓ requires two more harmonic polynomial basis functions and an enriched quadrature formula only on the boundary: indeed, an application of Green's theorem allows to compute the additional terms of (12) only by quadratures on faces.

Table 3: Values of σ_T computed with HHO$(k+1,k)$ on regular polygons. In parentheses, the value of ℓ.

k	$N_T^\partial = 3$	$N_T^\partial = 4$	$N_T^\partial = 5$	$N_T^\partial = 6$	$N_T^\partial = 7$
0	1.01e+00 (0)	9.50e-01 (0)	9.07e-01 (0)	7.83e-01 (0)	7.13e-01 (0)
1	3.34e-01 (0)	4.33e-01 (0)	4.62e-01 (1)	5.17e-01 (2)	5.18e-01 (3)
2	7.33e-02 (0)	8.94e-02 (1)	2.25e-01 (2)	2.51e-01 (4)	2.52e-01 (5)
k	$N_T^\partial = 8$	$N_T^\partial = 9$	$N_T^\partial = 10$	$N_T^\partial = 11$	$N_T^\partial = 12$
0	6.34e-01 (1)	5.81e-01 (1)	5.29e-01 (2)	4.90e-01 (2)	4.53e-01 (3)
1	4.99e-01 (4)	4.89e-01 (5)	4.60e-01 (6)	4.36e-01 (7)	4.11e-01 (8)
2	2.46e-01 (7)	2.78e-01 (8)	2.86e-01 (10)	2.61e-01 (11)	2.79e-01 (13)
k	$N_T^\partial = 13$	$N_T^\partial = 14$	$N_T^\partial = 15$	$N_T^\partial = 16$	$N_T^\partial = 17$
0	4.23e-01 (3)	3.96e-01 (4)	3.73e-01 (4)	3.51e-01 (5)	3.33e-01 (5)
1	3.90e-01 (9)	3.69e-01 (10)	3.51e-01 (11)	3.33e-01 (12)	3.18e-01 (13)
2	2.46e-01 (14)	2.63e-01 (16)	2.36e-01 (17)	2.51e-01 (19)	2.28e-01 (20)

Table 4: Concave polygons.

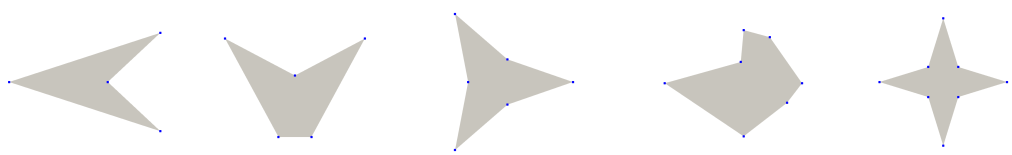

$N_T^\partial = 4$ $N_T^\partial = 5$ $N_T^\partial = 6$ $N_T^\partial = 7$ $N_T^\partial = 8$

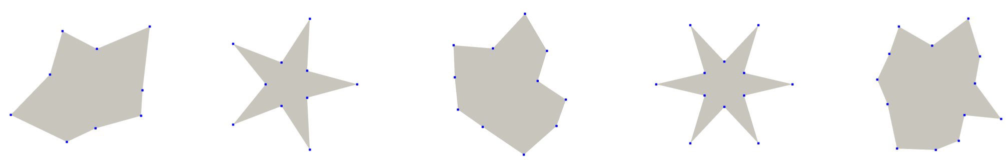

$N_T^\partial = 9$ $N_T^\partial = 10$ $N_T^\partial = 11$ $N_T^\partial = 12$ $N_T^\partial = 13$

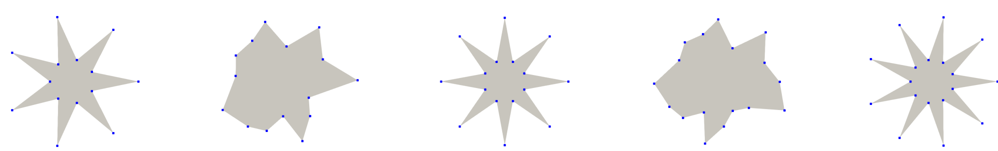

$N_T^\partial = 14$ $N_T^\partial = 15$ $N_T^\partial = 16$ $N_T^\partial = 17$ $N_T^\partial = 18$

Table 5: Values of σ_T computed with HHO$(k-1,k)$ on concave polygons. In parentheses, the value of ℓ.

k	$N_T^\partial = 4$	$N_T^\partial = 5$	$N_T^\partial = 6$	$N_T^\partial = 7$	$N_T^\partial = 8$
1	2.19e-03 (2)	6.88e-07 (3)	2.24e-01 (4)	1.67e-03 (5)	1.16e-01 (6)
2	3.26e-03 (3)	4.90e-04 (4)	8.59e-02 (6)	5.91e-06 (7)	3.48e-02 (9)
k	$N_T^\partial = 9$	$N_T^\partial = 10$	$N_T^\partial = 11$	$N_T^\partial = 12$	$N_T^\partial = 13$
1	2.74e-02 (7)	4.27e-02 (8)	6.20e-04 (9)	1.15e-02 (10)	1.58e-04 (11)
2	2.84e-04 (10)	1.25e-02 (12)	2.97e-07 (13)	3.07e-03 (15)	1.79e-07 (16)
k	$N_T^\partial = 14$	$N_T^\partial = 15$	$N_T^\partial = 16$	$N_T^\partial = 17$	$N_T^\partial = 18$
1	4.25e-03 (12)	2.50e-05 (13)	1.13e-03 (14)	7.46e-07 (15)	4.46e-04 (16)
2	8.59e-04 (18)	2.36e-08 (19)	1.98e-04 (21)	6.38e-10 (22)	6.21e-05 (24)

Table 6: Values of σ_T computed with HHO(k,k) on concave polygons. In parentheses, the value of ℓ.

k	$N_T^\partial = 4$	$N_T^\partial = 5$	$N_T^\partial = 6$	$N_T^\partial = 7$	$N_T^\partial = 8$
0	6.25e-01 (0)	3.96e-02 (0)	4.28e-01 (1)	8.92e-03 (1)	1.17e-01 (2)
1	1.62e-03 (1)	6.23e-07 (2)	2.08e-01 (3)	1.63e-03 (4)	1.16e-01 (5)
2	3.27e-03 (2)	4.80e-04 (3)	8.39e-02 (5)	5.87e-06 (6)	3.09e-02 (8)
k	$N_T^\partial = 9$	$N_T^\partial = 10$	$N_T^\partial = 11$	$N_T^\partial = 12$	$N_T^\partial = 13$
0	2.32e-01 (2)	5.87e-02 (3)	2.95e-02 (3)	1.92e-02 (4)	2.52e-02 (4)
1	2.72e-02 (6)	4.27e-02 (7)	6.02e-04 (8)	1.15e-02 (9)	1.56e-04 (10)
2	2.84e-04 (9)	6.01e-03 (11)	2.93e-07 (12)	1.82e-03 (14)	1.75e-07 (15)
k	$N_T^\partial = 14$	$N_T^\partial = 15$	$N_T^\partial = 16$	$N_T^\partial = 17$	$N_T^\partial = 18$
0	9.53e-03 (5)	4.78e-03 (5)	2.88e-03 (6)	1.31e-03 (6)	1.40e-03 (7)
1	4.25e-03 (11)	2.46e-05 (12)	1.13e-03 (13)	7.40e-07 (14)	4.46e-04 (15)
2	7.00e-04 (17)	2.23e-08 (18)	1.98e-04 (20)	6.37e-10 (21)	6.21e-05 (23)

Table 7: Values of σ_T computed with HHO$(k+1,k)$ on concave polygons. In parentheses, the value of ℓ.

k	$N_T^\partial = 4$	$N_T^\partial = 5$	$N_T^\partial = 6$	$N_T^\partial = 7$	$N_T^\partial = 8$
0	3.54e-01 (0)	3.91e-01 (0)	3.36e-01 (0)	3.20e-02 (0)	1.17e-01 (1)
1	2.92e-02 (0)	2.21e-03 (1)	1.55e-01 (2)	4.07e-03 (3)	5.07e-02 (4)
2	2.53e-10 (1)	3.56e-03 (2)	2.78e-02 (4)	1.22e-07 (5)	3.13e-03 (7)
k	$N_T^\partial = 9$	$N_T^\partial = 10$	$N_T^\partial = 11$	$N_T^\partial = 12$	$N_T^\partial = 13$
0	2.37e-01 (1)	5.87e-02 (2)	2.66e-02 (2)	1.92e-02 (3)	3.13e-02 (3)
1	2.57e-02 (5)	6.34e-03 (6)	8.85e-04 (7)	1.47e-03 (8)	3.66e-04 (9)
2	2.57e-04 (8)	3.76e-03 (10)	1.45e-10 (11)	1.35e-03 (13)	1.38e-06 (14)
k	$N_T^\partial = 14$	$N_T^\partial = 15$	$N_T^\partial = 16$	$N_T^\partial = 17$	$N_T^\partial = 18$
0	9.53e-03 (4)	4.44e-03 (4)	2.88e-03 (5)	3.09e-03 (5)	1.40e-03 (6)
1	4.49e-04 (10)	1.38e-04 (11)	1.93e-04 (12)	3.38e-07 (13)	1.22e-04 (14)
2	2.32e-04 (16)	6.41e-09 (17)	9.60e-05 (19)	1.07e-08 (20)	6.21e-05 (22)

Table 8: Values of σ_T computed with HHO$(k-1,k)$ on polygons with aligned edges. In parentheses, the value of ℓ.

k	$N_T^\partial = 5$	$N_T^\partial = 6$	$N_T^\partial = 7$	$N_T^\partial = 8$	$N_T^\partial = 9$
1	2.54e-02 (3)	1.82e-02 (4)	1.74e-01 (5)	4.70e-01 (6)	1.81e-02 (7)
2	8.88e-05 (4)	1.57e-04 (6)	9.93e-05 (7)	2.03e-01 (9)	3.80e-05 (10)
k	$N_T^\partial = 10$	$N_T^\partial = 11$	$N_T^\partial = 12$	$N_T^\partial = 13$	$N_T^\partial = 14$
1	1.24e-02 (8)	7.57e-02 (9)	2.99e-01 (10)	8.15e-03 (11)	6.31e-03 (12)
2	1.01e-04 (12)	6.43e-05 (13)	6.43e-02 (15)	9.03e-06 (16)	3.62e-05 (18)

Table 9: Values of σ_T computed with HHO(k,k) on polygons with aligned edges. In parentheses, the value of ℓ.

k	$N_T^\partial = 5$	$N_T^\partial = 6$	$N_T^\partial = 7$	$N_T^\partial = 8$	$N_T^\partial = 9$
0	1.83e-01 (0)	6.67e-01 (1)	2.75e-01 (1)	6.94e-01 (2)	1.88e-01 (2)
1	2.54e-02 (2)	1.82e-02 (3)	1.74e-01 (4)	4.13e-01 (5)	1.81e-02 (6)
2	8.88e-05 (3)	1.57e-04 (5)	9.93e-05 (6)	1.98e-01 (8)	3.80e-05 (9)
k	$N_T^\partial = 10$	$N_T^\partial = 11$	$N_T^\partial = 12$	$N_T^\partial = 13$	$N_T^\partial = 14$
0	3.97e-01 (3)	2.08e-01 (3)	4.61e-01 (4)	1.42e-01 (4)	3.05e-01 (5)
1	1.24e-02 (7)	7.57e-02 (8)	2.88e-01 (9)	8.15e-03 (10)	6.31e-03 (11)
2	1.01e-04 (11)	6.43e-05 (12)	6.43e-02 (14)	9.03e-06 (15)	3.62e-05 (17)

Table 10: Values of σ_T computed with HHO$(k+1,k)$ on polygons with aligned edges. In parentheses, the value of ℓ.

k	$N_T^\partial = 5$	$N_T^\partial = 6$	$N_T^\partial = 7$	$N_T^\partial = 8$	$N_T^\partial = 9$
0	6.96e-01 (0)	5.90e-01 (0)	2.89e-01 (0)	5.19e-01 (1)	1.88e-01 (1)
1	2.54e-02 (1)	1.95e-02 (2)	1.74e-01 (3)	3.68e-01 (4)	1.81e-02 (5)
2	9.09e-05 (2)	1.66e-04 (4)	1.05e-04 (5)	8.75e-02 (7)	3.80e-05 (8)
k	$N_T^\partial = 10$	$N_T^\partial = 11$	$N_T^\partial = 12$	$N_T^\partial = 13$	$N_T^\partial = 14$
0	3.86e-01 (2)	2.07e-01 (2)	3.76e-01 (3)	1.42e-01 (3)	2.97e-01 (4)
1	1.21e-02 (6)	7.57e-02 (7)	2.87e-01 (8)	8.15e-03 (9)	6.26e-03 (10)
2	1.01e-04 (10)	6.43e-05 (11)	6.39e-02 (13)	9.02e-06 (14)	3.61e-05 (16)

4.1.3 Polygons with aligned edges

Finally, we consider a sequence of convex polygons with aligned edges obtained starting from a square and then splitting its edges into equal parts, one edge at each step until we obtain a polygon with 14 edges. In Tables 8, 9 and 10 we display the values of σ_T of the elemental stiffness matrix obtained applying the three methods discussed, respectively, and the related value of the polynomial incremental degree ℓ, determined according to (23). Also in this case, we notice that we have obtained the numerical stability applying the necessary condition on ℓ.

4.1.4 Polyhedra

In the 3D setting we consider a mesh composed of 48 tetrahedra with different aspect ratios, a mesh of prisms obtained from the FVCA6 benchmark featuring some heavily distorted elements (Figure 1), and a cube. For each mesh, a unique value $\ell^\star$ is chosen in such a way that the local reconstruction on $\tilde{\mathbb{P}}_3^{k',\ell^\star}(T)$ is observed to be coercive for all elements T.

For each element T of each mesh, we consider the value of σ_T/h_T, which is invariant with respect to rescalings of T. In Table 11, for all the variants of the proposed HHO method, we report the maximum and minimum numerical value of σ_T/h_T computed on the tetrahedral mesh, together with the minimum value ℓ satisfying the necessary condition (24), and the value $\ell^\star$ observed to guarantee local coercivity. In Table 12 the same results are shown for the prismatic mesh, and in Table 13 we report the results on the cubic element. We remark that in some cases $\ell^\star > \ell$ is needed. A better investigation of the 3D setting is left for a future work.

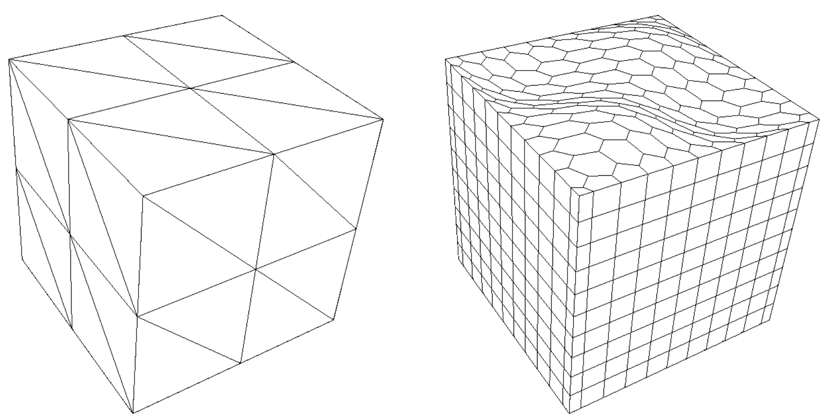

Figure 1: Meshes of the unit cube used to test the stability in 3D. The tetrahedral mesh on the left is composed of 48 elements and was generated internally by DiSk++, whereas the prismatic mesh on the right is the “DBLS10” mesh from the FVCA6 benchmark.

Table 11: Minimum and maximum values of σ_T/h_T on the tetrahedral mesh, with a comparison between the numerically required and theoretically necessary degrees of enrichment.

HHO($k-1$,k)	min σ_T/h_T	max σ_T/h_T	$\ell^\star$	ℓ
$k=1$	1.26E-02	5.03E-02	1	1
$k=2$	4.28E-04	1.72E-02	1	1
HHO(k, k)	min σ_T/h_T	max σ_T/h_T	$\ell^\star$	ℓ
$k=0$	1.95E-01	1.06E+00	0	0
$k=1$	1.13E-02	4.48E-02	0	0
$k=2$	3.94E-04	1.66E-02	0	0
HHO($k+1$, k)	min σ_T/h_T	max σ_T/h_T	$\ell^\star$	ℓ
$k=0$	4.78E-02	2.90E-01	0	0
$k=1$	3.49E-03	3.05E-02	0	0
$k=2$	1.03E-04	1.73E-03	0	0

Table 12: Minimum and maximum values of σ_T/h_T on the prismatic mesh, with a comparison between the numerically required and theoretically necessary degrees of enrichment, chosen to guarantee the stability on all the mesh elements (see text).

HHO($k-1$,k)	min σ_T/h_T	max σ_T/h_T	$\ell^\star$	ℓ
$k=1$	5.64E-05	1.22E-01	3	2
$k=2$	3.76E-07	8.19E-02	4	3
HHO(k, k)	min σ_T/h_T	max σ_T/h_T	$\ell^\star$	ℓ
$k=0$	1.11E-01	5.29E-01	1	0
$k=1$	5.64E-05	1.08E-01	2	1
$k=2$	3.74E-07	8.06E-02	3	2
HHO($k+1$, k)	min σ_T/h_T	max σ_T/h_T	$\ell^\star$	ℓ
$k=0$	7.92E-02	3.83E-01	0	0
$k=1$	3.38E-02	1.97E-01	2	0
$k=2$	3.74E-07	7.04E-02	2	1

4.2 Convergence tests

We now consider the model problem in the unit hypercube $\Omega = [0,1]^d$, with $d = 2,3$, choosing the source term f such that the solution is $u(\mathbf{x}) = \prod_{i=1}^{d} \sin(\pi x_i)$. We investigate the rates of convergence of the errors in the discrete energy norm and the L^2-norm, estimated in Theorems 1 and 2 for the proposed methods. The value of ℓ is chosen according to the above discussions. Moreover, we compare the stabilization-free methods with the standard stabilized HHO methods. In Figures 2, 3 and 4 we show the errors with HHO methods of order $k \in \{0,1,2\}$ for tesselations of triangles, squares and hexagons, respectively. In addition, we show in Figures 5, 6 and 7 the errors with HHO methods of order $k \in \{0,1,2\}$ for tetrahedras, cubic and prismatic meshes (see Fig. 1), respectively. In all cases, the numerical data are in agreement with the convergences rates expected from the theory. Let us add two additional observations from these figures. For the HHO($k-1,k$) method we observe very close profiles, even overlapping with the standard stabilized results. For HHO(k,k) and HHO($k+1,k$), the stabilization-free scheme shows smaller approximation errors. The most outstanding differences can be seen in Figure 4 for the 2D-case and in Figures 6, 7 for the 3D-case. More precisely, we remark that this gap grows to one order and even two orders of magnitude in the energy norm (right panel) and in the L^2-error (left panel), respectively.

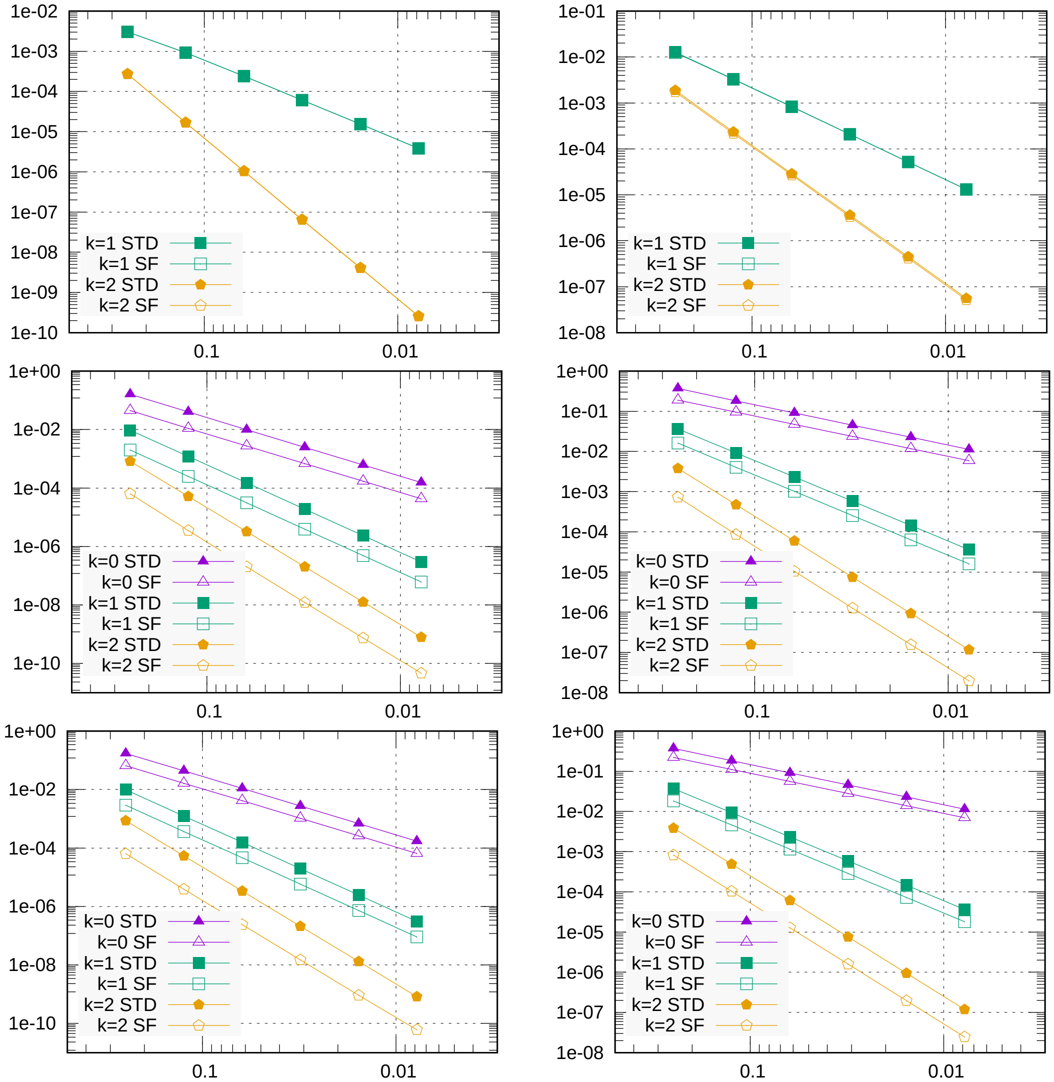

Figure 2: Convergence data on triangular meshes. From the top to the bottom: HHO$(k-1,k)$, HHO(k,k) and HHO$(k+1,k)$. On the left the L^2-norm error, on the right the discrete energy error. STD: standard HHO; SF: proposed stabilization-free methods.

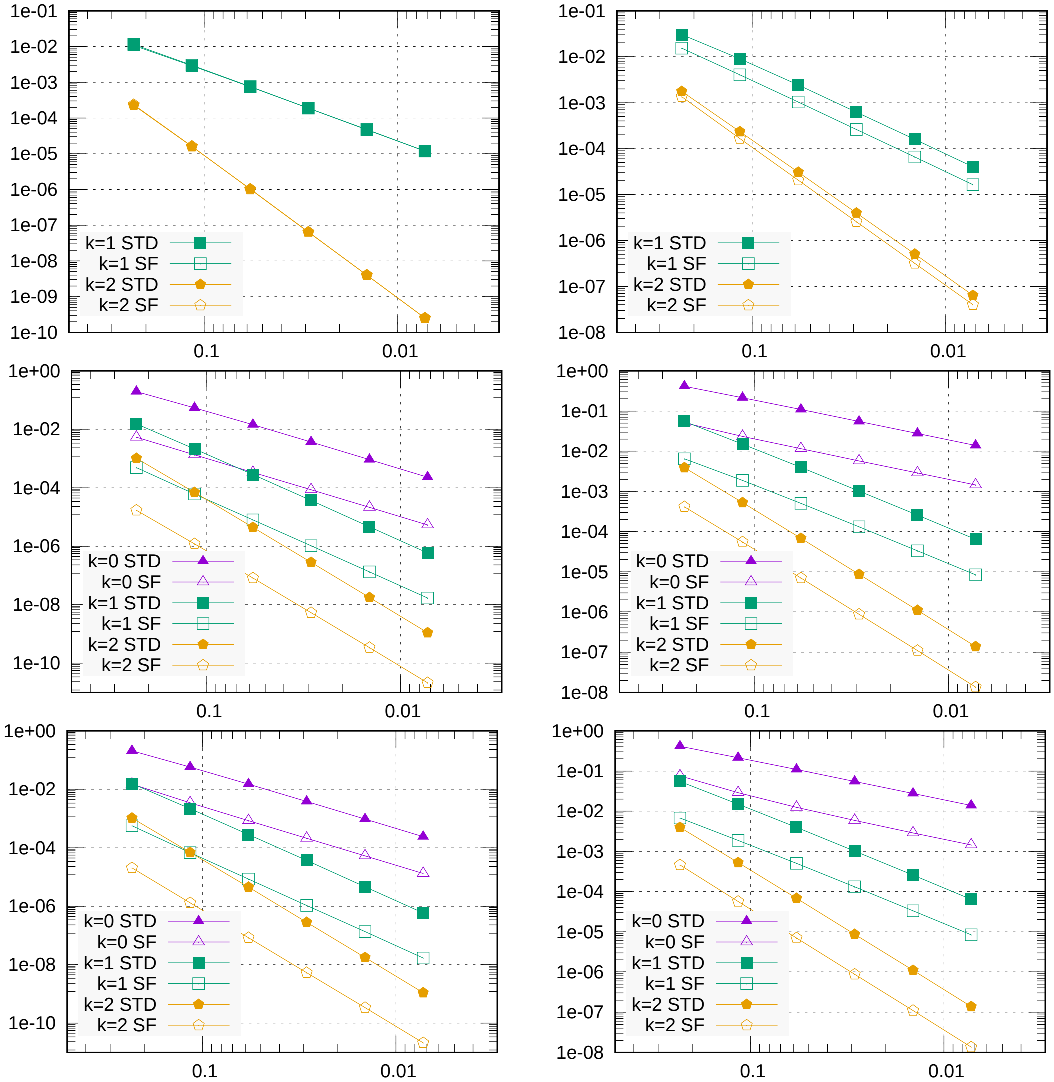

Figure 3: Convergence data on meshes of squares. From the top to the bottom: HHO$(k-1, k)$, HHO(k, k) and HHO$(k+1, k)$. On the left the L^2-norm error, on the right the discrete energy error. STD: standard HHO; SF: proposed stabilization-free methods.

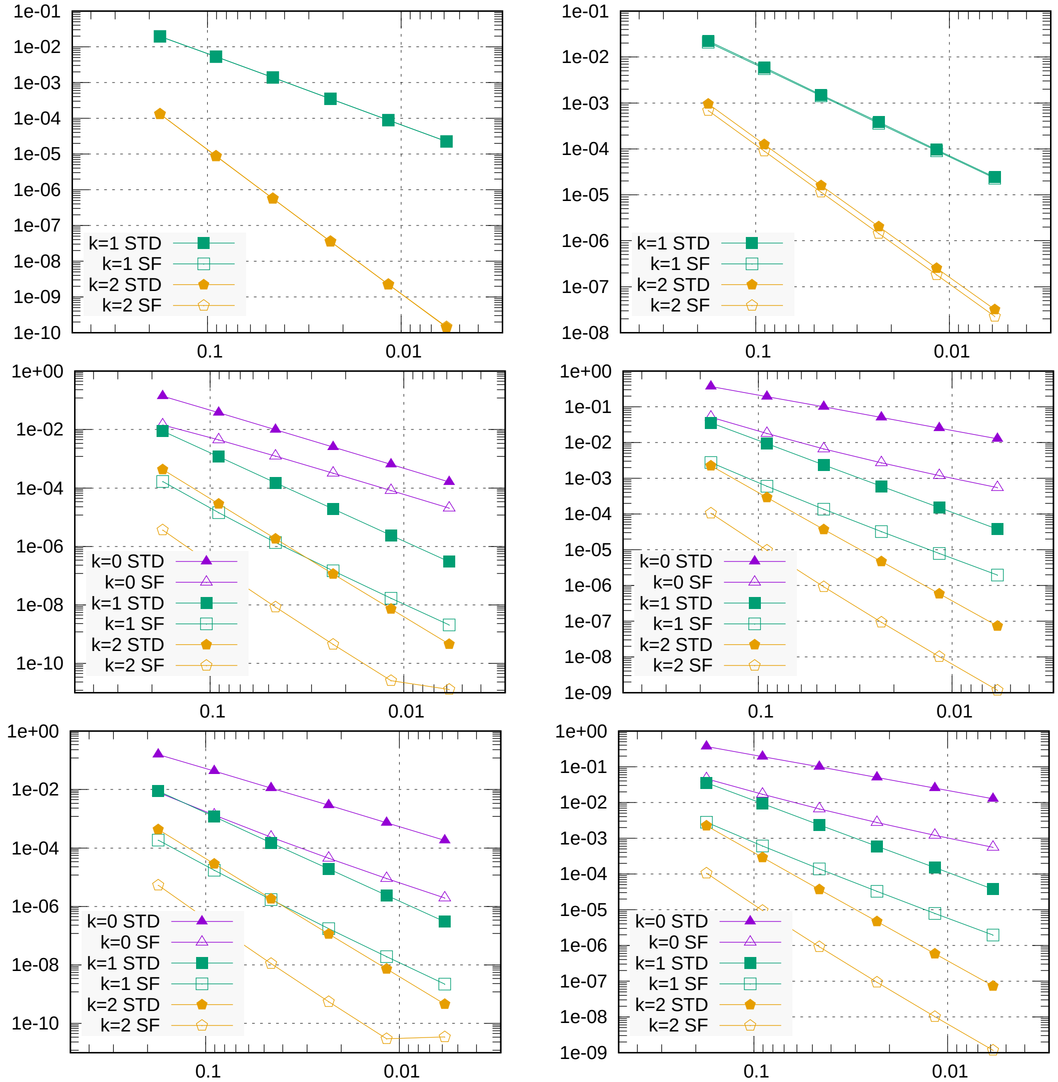

Figure 4: Convergence data on hex-dominant meshes. From the top to the bottom: HHO$(k-1,k)$, HHO(k,k) and HHO$(k+1,k)$. On the left the L^2-norm error, on the right the discrete energy error. STD: standard HHO; SF: proposed stabilization-free methods.

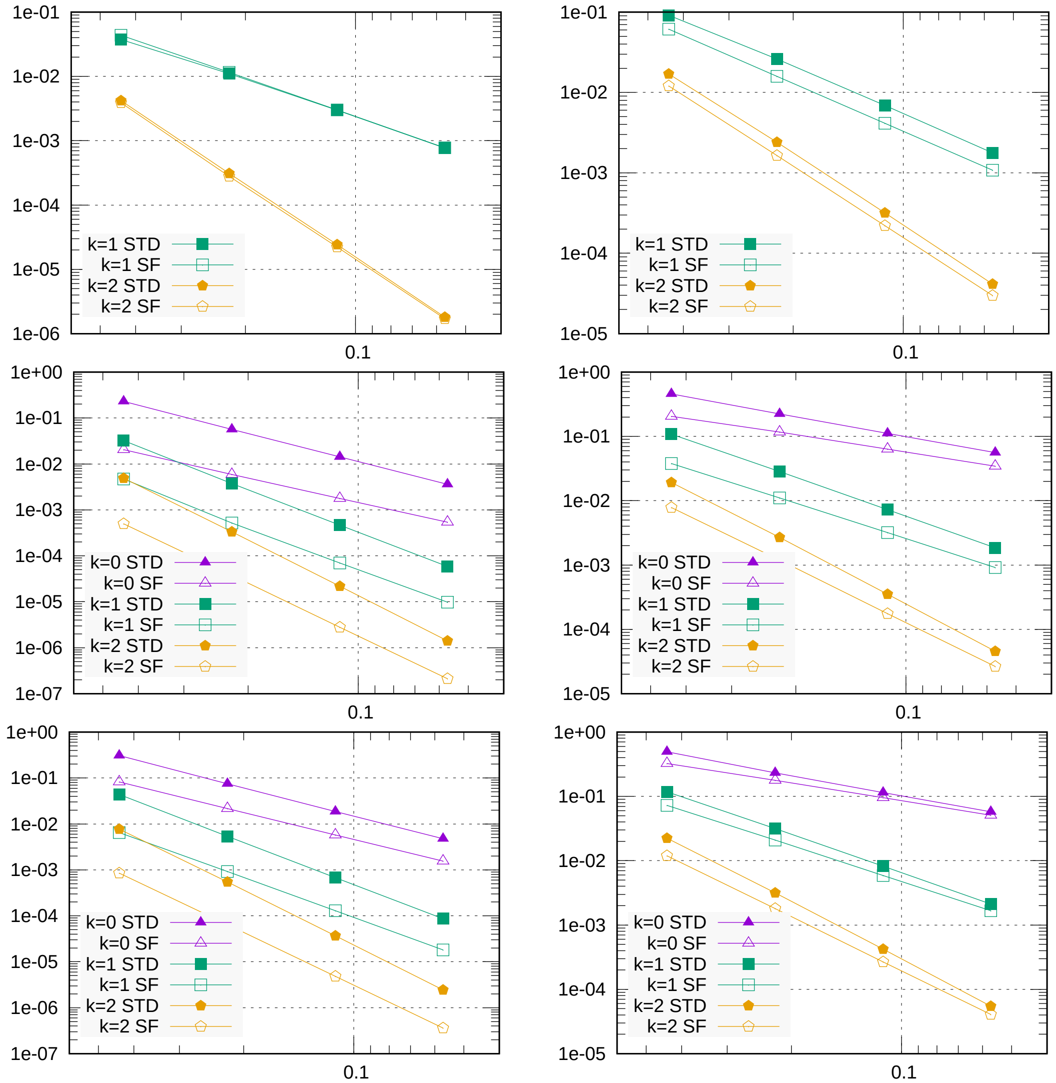

Figure 5: Convergence data on tetrahedral meshes. From the top to the bottom: HHO$(k-1,k)$, HHO(k,k) and HHO$(k+1,k)$. On the left the L^2-norm error, on the right the discrete energy error. STD: standard HHO; SF: proposed stabilization-free methods.

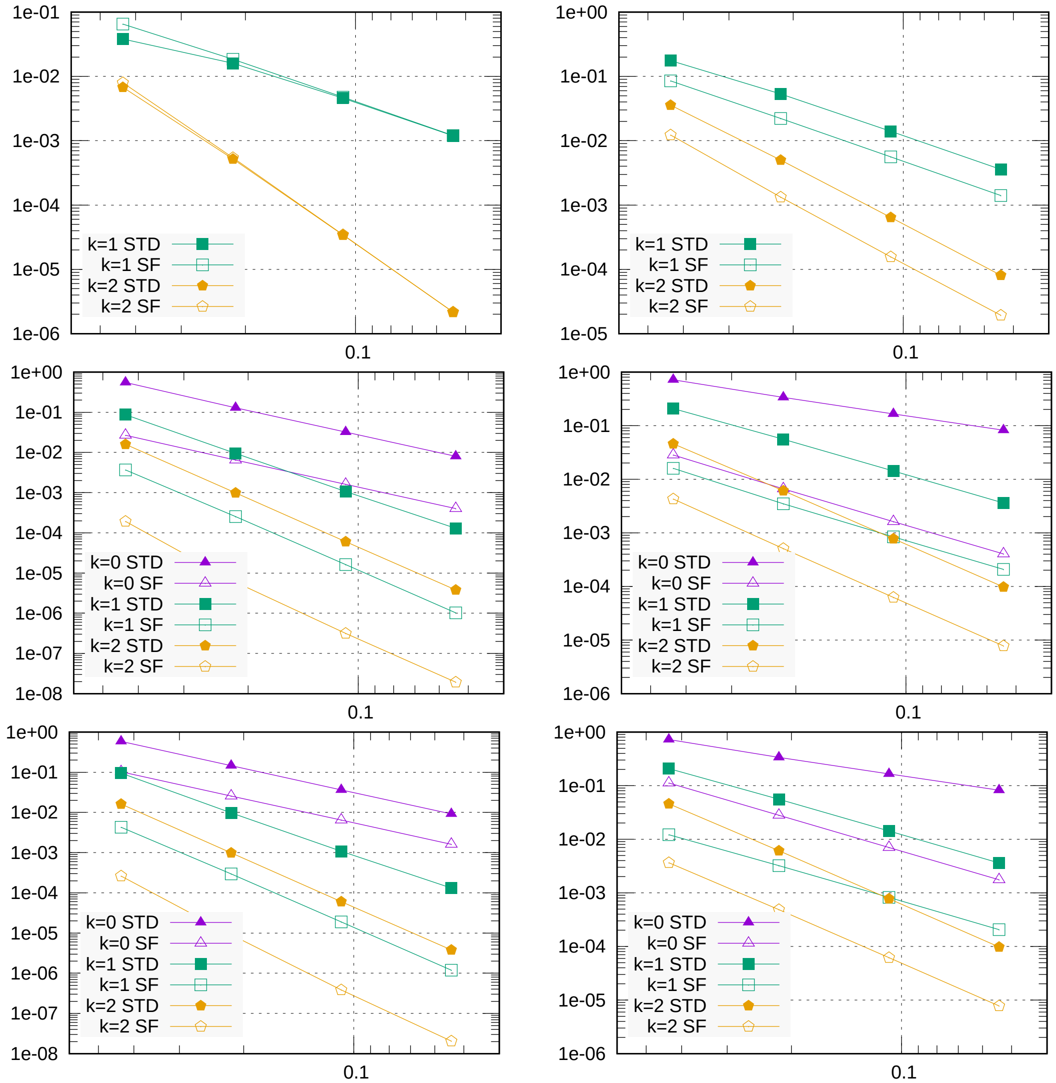

Figure 6: Convergence data on meshes of cubes. From the top to the bottom: HHO$(k-1,k)$, HHO(k,k) and HHO$(k+1,k)$. On the left the L^2-norm error, on the right the discrete energy error. STD: standard HHO; SF: proposed stabilization-free methods.

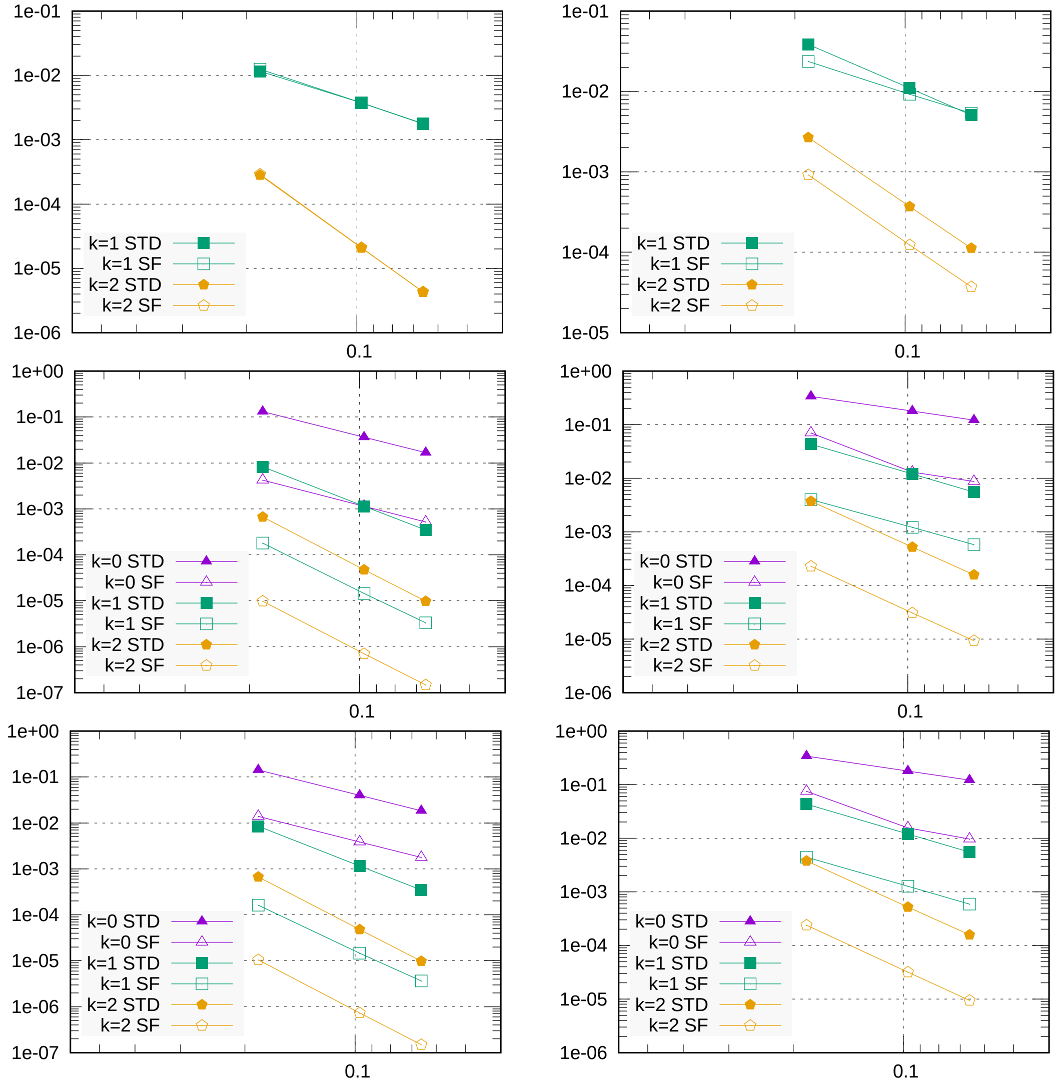

Figure 7: Convergence data on FVCA6 DBLS meshes. From the top to the bottom: HHO$(k-1,k)$, HHO(k,k) and HHO$(k+1,k)$. On the left the L^2-norm error, on the right the discrete energy error. STD: standard HHO; SF: proposed stabilization-free methods.

Table 13: Values of σ_T/h_T on the cubic element, with a comparison between the numerically required and theoretically necessary degrees of enrichment.

HHO($k-1$,k)	σ_T/h_T	$\ell^\star$	ℓ
$k=1$	0.273565	2	2
$k=2$	0.1283	3	2
HHO(k, k)	σ_T/h_T	$\ell^\star$	ℓ
$k=0$	1.1547	0	0
$k=1$	0.246236	1	1
$k=2$	0.1283	2	1
HHO($k+1$, k)	σ_T/h_T	$\ell^\star$	ℓ
$k=0$	0.752323	0	0
$k=1$	0.246236	0	0
$k=2$	0.109433	1	0

5 Conclusions

Novel stabilization-free Hybrid High-Order methods were introduced for solving elliptic problems. The methods were formulated for Poisson's equation and are based on local reconstruction operators mapping discrete HHO variables on suitably enriched polynomial spaces. The well-posedness of the discrete schemes was explored numerically through an extensive campaign of tests on polygons and polyhedra. In 2D, results suggest that the new reconstruction operators are stable provided that the dimension of the reconstruction space is greater than the dimension of the local HHO spaces. In 3D, results suggest that it is possible to choose a value of the polynomial enrichment degree ℓ providing coercivity, however this may be higher than the one resulting from simple considerations on space dimensions. Optimal order a priori error estimates are proved whenever reconstruction operators are locally stable. In some cases, convergence tests display a significant reduction of the magnitude of the error with respect to the standard, stabilized HHO method. Future works will address the issue of well-posedness from the theoretical point of view, with the aim of identifying sufficient conditions on the reconstruction space guaranteeing stability.

Acknowledgements

The four authors are members of the Gruppo Nazionale Calcolo Scientifico (GNCS) at Istituto Nazionale di Alta Matematica (INdAM). The authors acknowledge financial support by INdAM-GNCS Projects 2024 (CUP: E53C23001670001) and 2025 (CUP: E53C24001950001), by the Italian Ministry of University and Research (MUR) through the project MUR-M4C2-1.1-PRIN 2022 (CUP: E53D23005820006), and by the European Union through Next Generation EU, M4C2, PRIN 2022 PNRR project (CUP: E53D23017950001) and PNRR M4C2 project of CN00000013 National Centre for HPC, Big Data and Quantum Computing (HPC) (CUP: E13C22000990001). Finally, we thank the anonymous reviewers for their insightful comments and suggestions, which helped us to improve the quality of the manuscript.

Conflict of interest

The authors declare that they have no conflict of interest.

Data availability

Data will be made available on request.

References

[1] Abbas, M., Ern, A., Pignet, N.: Hybrid High-Order methods for finite deformations of hyperelastic materials. Comput. Mech. **62**(4), 909–928 (2018). DOI 10.1007/s00466-018-1538-0

[2] Berrone, S., Borio, A., Fassino, D., Marcon, F.: Stabilization-free Virtual Element Method for 2D second order elliptic equations. Computer Methods in Applied Mechanics and Engineering **438**, 117839 (2025). DOI 10.1016/j.cma.2025.117839

[3] Berrone, S., Borio, A., Marcon, F.: A stabilization-free virtual element method based on divergence-free projections. Computer Methods in Applied Mechanics and Engineering **424**, 116885 (2024). DOI 10.1016/j.cma.2024.116885

[4] Berrone, S., Borio, A., Marcon, F.: Lowest order stabilization free virtual element method for the 2D Poisson equation. Computers and Mathematics with Applications **177**, 78–99 (2025). DOI 10.1016/j.camwa.2024.11.017

[5] Berrone, S., Borio, A., Marcon, F., Teora, G.: A first-order stabilization-free Virtual Element Method. Applied Mathematics Letters **142**, 108641 (2023). DOI 10.1016/j.aml.2023.108641

[6] Boffi, D., Gardini, F., Gastaldi, L.: Approximation of PDE eigenvalue problems involving parameter dependent matrices. Calcolo **57**(4), 41 (2020). DOI 10.1007/s10092-020-00390-6

[7] Boffi, D., Gardini, F., Gastaldi, L.: Virtual Element Approximation of Eigenvalue Problems. In: P.F. Antonietti, L. Beirão Da Veiga, G. Manzini (eds.) The Virtual Element Method and its Applications, vol. 31, pp. 275–320. Springer International Publishing, Cham (2022). DOI 10.1007/978-3-030-95319-5_7. Series Title: SEMA SIMAI Springer Series

[8] Borio, A., Busetto, M., Marcon, F.: SUPG-stabilized stabilization-free VEM: a numerical investigation. Mathematics in Engineering **6**(1), 173–191 (2024). DOI 10.3934/mine.2024008

[9] Botti, L., Di Pietro, D.A., Droniou, J.: A Hybrid High-Order method for the incompressible Navier-Stokes equations based on Temam's device. J. Comput. Phys. **376**, 786–816 (2019). DOI 10.1016/j.jcp.2018.10.014

[10] Botti, M., Di Pietro, D.A., Sochala, P.: A Hybrid High-Order discretization method for nonlinear poroelasticity. Comput. Methods Appl. Math. **20**(2), 227–249 (2020). DOI 10.1515/cmam-2018-0142

[11] Burman, E., Cicuttin, M., Delay, G., Ern, A.: An unfitted Hybrid High-Order method with cell agglomeration for elliptic interface problems. SIAM J. Sci. Comput. **43**(2), A859–A882 (2021). DOI 10.1137/19M1285901

[12] Burman, E., Duran, O., Ern, A.: Hybrid High-Order Methods for the Acoustic Wave Equation in the Time Domain. Communications on Applied Mathematics and Computation **4**(2), 597–633 (2022). DOI 10.1007/s42967-021-00131-8

[13] Bustinza, R., Cicuttin, M., Lombardi, A.: A hybrid high-order method for the mixed Steklov eigenvalue problem. Numerische Mathematik **157**, 447–475 (2025). DOI 10.1007/s00211-025-01463-w

[14] Calo, V., Cicuttin, M., Deng, Q., Ern, A.: Spectral approximation of elliptic operators by the hybrid high-order method. Mathematics of computation **88**(318), 1559–1586 (2019). DOI 10.1090/mcom/3405

[15] Cascavita, K.L., Bleyer, J., Chateau, X., Ern, A.: Hybrid discretization methods with adaptive yield surface detection for Bingham pipe flows. J. Sci. Comput. **77**(3), 1424–1443 (2018). DOI 10.1007/s10915-018-0745-3

[16] Cascavita, K.L., Chouly, F., Ern, A.: Hybrid High-Order discretizations combined with Nitsche's method for Dirichlet and Signorini boundary conditions. IMA J. Numer. Anal. **40**(4), 2189–2226 (2020). DOI 10.1093/imanum/drz038

[17] Chave, F., Di Pietro, D.A., Formaggia, L.: A Hybrid High-Order Method for Darcy Flows in Fractured Porous Media. SIAM Journal on Scientific Computing **40**(2), A1063–A1094 (2018). DOI 10.1137/17M1119500

[18] Chave, F., Di Pietro, D.A., Lemaire, S.: A discrete Weber inequality on three-dimensional hybrid spaces with application to the HHO approximation of magnetostatics. Mathematical Models and Methods in Applied Sciences **32**(01), 175–207 (2022). DOI 10.1142/S0218202522500051

[19] Chen, A., Sukumar, N.: Stabilization-free virtual element method for plane elasticity. Computers & Mathematics with Applications **138**, 88–105 (2023). DOI 10.1016/j.camwa.2023.03.002

[20] Cicuttin, M.: An implementation detail about the scaling of monomial bases in polytopal finite element methods. Applied Mathematics Letters **159**, 109281 (2025). DOI 10.1016/j.aml.2024.109281

[21] Cicuttin, M., Di Pietro, D.A., Ern, A.: Implementation of Discontinuous Skeletal methods on arbitrary-dimensional, polytopal meshes using generic programming. Journal of Computational and Applied Mathematics **344**, 852–874 (2018). DOI 10.1016/j.cam.2017.09.017

[22] Cicuttin, M., Ern, A., Gudi, T.: Hybrid High-Order methods for the elliptic obstacle problem. J. Sci. Comput. **83**(1), Paper No. 8, 18 (2020). DOI 10.1007/s10915-020-01195-z

[23] Cicuttin, M., Ern, A., Lemaire, S.: A Hybrid High-Order method for highly oscillatory elliptic problems. Comput. Methods Appl. Math. **19**(4), 723–748 (2019). DOI 10.1515/cmam-2018-0013

[24] Cicuttin, M., Ern, A., Pignet, N.: Hybrid High-Order Methods: A Primer with Applications to Solid Mechanics. Springer International Publishing, Cham (2021). DOI 10.1007/978-3-030-81477-9_3

[25] Cicuttin, M., Geuzaine, C.: Numerical investigation of a 3D Hybrid High-Order method for the indefinite time-harmonic Maxwell problem. Finite Elements in Analysis and Design **233**, 104124 (2024). DOI 10.1016/j.finel.2024.104124

[26] Cockburn, B.: Static condensation, hybridization, and the devising of the HDG methods. In: G.R. Barrenechea, F. Brezzi, A. Cangiani, E.H. Georgoulis (eds.) Building Bridges: Connections and Challenges in Modern Approaches to Numerical Partial Differential Equations, *Lecture Notes in Computational Science and Engineering*, vol. 114, pp. 129–178. Springer, Switzerland (2016). DOI 10.1007/978-3-319-41640-3_5

[27] Cockburn, B., Di Pietro, D.A., Ern, A.: Bridging the Hybrid High-Order and hybridizable discontinuous Galerkin methods. ESAIM Math. Model. Numer. Anal. **50**(3), 635–650 (2016). DOI 10.1051/m2an/2015051

[28] Di Pietro, D.A., Droniou, J.: The Hybrid High-Order method for polytopal meshes, *Modeling, Simulation and Application*, vol. 19. Springer International Publishing (2020). DOI 10.1007/978-3-030-37203-3

[29] Di Pietro, D.A., Droniou, J., Manzini, G.: Discontinuous Skeletal Gradient Discretisation methods on polytopal meshes. Journal of Computational Physics **355**, 397–425 (2018). DOI 10.1016/j.jcp.2017.11.018

[30] Di Pietro, D.A., Ern, A.: A Hybrid High-Order locking-free method for linear elasticity on general meshes. Computer Methods in Applied Mechanics and Engineering **283**, 1–21 (2015). DOI 10.1016/j.cma.2014.09.009

[31] Di Pietro, D.A., Ern, A., Lemaire, S.: An Arbitrary-Order and Compact-Stencil Discretization of Diffusion on General Meshes Based on Local Reconstruction Operators. Computational Methods in Applied Mathematics **14**(4), 461–472 (2014). DOI doi:10.1515/cmam-2014-0018

[32] Droniou, J., Eymard, R., Gallouët, T., Herbin, R.: A unified approach to mimetic finite difference, hybrid finite volume and mixed finite volume methods. Math. Models Methods Appl. ScM. **20**(2), 265–295 (2010). DOI 10.1142/S0218202510004222

[33] D'Altri, A., de Miranda, S., Patruno, L., Sacco, E.: An enhanced VEM formulation for plane elasticity. Computer Methods in Applied Mechanics and Engineering **376**, 113663 (2021). DOI 10.1016/j.cma.2020.113663

[34] Ern, A., Guermond, J.L.: Quasi-optimal nonconforming approximation of elliptic pdes with contrasted coefficients and h^{1+r}, $r > 0$, regularity. Foundations of computational mathematics **22**(5), 1273–1308 (2022). DOI 10.1007/s10208-021-09527-7

[35] Eymard, R., Gallouët, T., Herbin, R.: Discretization of heterogeneous and anisotropic diffusion problems on general nonconforming meshes SUSHI: a scheme using stabilization and hybrid interfaces. IMA J. Numer. Anal. **30**(4), 1009–1043 (2010). DOI 10.1093/imanum/drn084

[36] Grisvard, P.: Elliptic Problems in Nonsmooth Domains. Society for Industrial and Applied Mathematics (2011). DOI 10.1137/1.9781611972030

[37] John, L., Neilan, M., Smears, I.: Stable Discontinuous Galerkin FEM Without Penalty Parameters. In: B. Karasözen, M. Manguoğlu, M. Tezer-Sezgin, S. Göktepe, Ö. Uğur (eds.) Numerical Mathematics and Advanced Applications ENUMATH 2015, pp. 165–173. Springer International Publishing, Cham (2016). DOI 10.1007/978-3-319-39929-4_17

[38] Lamperti, A., Cremonesi, M., Perego, U., Lovadina, C., Russo, A.: A Hu-Washizu variational approach to self-stabilized Virtual Elements: 2D linear elastostatics. Computational Mechanics **71**, 935–955 (2023). DOI 10.1007/s00466-023-02282-2

[39] Lemaire, S.: Bridging the Hybrid High-Order and Virtual Element Methods. IMA Journal of Numerical Analysis **41**(1), 549–593 (2021). DOI 10.1093/imanum/drz056

[40] Marcon, F., Mora, D.: A Stabilization-Free Virtual Element Method for the Convection–Diffusion Eigenproblem. Journal of Scientific Computing **102**(2), 46 (2025). DOI 10.1007/s10915-024-02765-1

[41] Xu, B.B., Peng, F., Wriggers, P.: Stabilization-free virtual element method for finite strain applications. Computer Methods in Applied Mechanics and Engineering **417**, 116555 (2023). DOI 10.1016/j.cma.2023.116555

[42] Ye, X., Zhang, S.: A stabilizer free weak Galerkin finite element method on polytopal mesh: Part II. Journal of Computational and Applied Mathematics **394**, 113525 (2021). DOI 10.1016/j.cam.2021.113525